

## On the Lefkas (Ionian Sea) November 17, 2015 Mw=6.5 Earthquake Macroseismic Effects

Ioannis Kassaras, Danai Kazantzidou-Firtinidou, Athanassios Ganas, Sandra Tonna, Antonios Pomonis, Christos Karakostas, Chara Papadatou-Giannopoulou, Dimitrios Psarris, Efthymios Lekkas & Konstantinos Makropoulos

To cite this article: Ioannis Kassaras, Danai Kazantzidou-Firtinidou, Athanassios Ganas, Sandra Tonna, Antonios Pomonis, Christos Karakostas, Chara Papadatou-Giannopoulou, Dimitrios Psarris, Efthymios Lekkas & Konstantinos Makropoulos (2018): On the Lefkas (Ionian Sea) November 17, 2015 Mw=6.5 Earthquake Macroseismic Effects, Journal of Earthquake Engineering

To link to this article: <https://doi.org/10.1080/13632469.2018.1488776>



Published online: 23 Jul 2018.




Submit your article to this journal [↗](#)



View Crossmark data [↗](#)



# On the Lefkas (Ionian Sea) November 17, 2015 Mw=6.5 Earthquake Macroseismic Effects

Ioannis Kassaras <sup>a</sup>, Danai Kazantzidou-Firtinidou<sup>a</sup>, Athanassios Ganas<sup>b</sup>, Sandra Tonna<sup>c</sup>, Antonios Pomonis<sup>d</sup>, Christos Karakostas<sup>e</sup>, Chara Papadatou-Giannopoulou<sup>f</sup>, Dimitrios Psarris<sup>a</sup>, Efthymios Lekkas<sup>a</sup>, and Konstantinos Makropoulos<sup>a</sup>

<sup>a</sup>Department of Geophysics-Geothermics, Laboratory of Seismology, National and Kapodistrian University of Athens, Athens, Greece; <sup>b</sup>Institute of Geodynamics, National Observatory of Athens, Athens, Greece; <sup>c</sup>A.B.C. Dep., Politecnico di Milano, Milan, Italy; <sup>d</sup>Cambridge Architectural Research Limited, Cambridge, United Kingdom; <sup>e</sup>Department of Earthquake Engineering, EPPO-ITSAK, Thessaloniki, Greece; <sup>f</sup>Freelancer, Maizonos 14, Patras, Greece

## ABSTRACT

We exploit macroseismic observations and instrumental data aiming at explaining the effects of the 17th November 2015 Mw=6.5 earthquake, occurred beneath the southwestern peninsula of Lefkas Island (Ionian Sea) causing two casualties, major geo-environmental and slight-to-moderate structural effects. The spatial distribution of the structural damage of the local building stock is well correlated with the deformation pattern deduced from satellite geodesy, it appears though considerably low with respect to the ground deformation. Comparison with the previous strong earthquake on 14.8.2003 with Mw=6.2 occurred about 20 km to the north, shows that structural damage was significantly lower during the recent quake and also manifests good behaviour of the local buildings. This is partly explained by the characteristics of the ground motion and primarily explained by the unique concepts applied to the non-engineered buildings of Lefkas to resist ground motions.

## ARTICLE HISTORY

Received 10 January 2017  
Accepted 6 June 2018

## KEYWORDS

Seismic Damage; Seismic Vulnerability; Non-Engineered Buildings; Pontelo; Lefkas

## 1. Introduction

We investigate the macroseismic effects of the November 17, 2015 Mw = 6.5 Lefkas earthquake focused on the endurance of the Lefkas non-engineered traditional constructions toward the ground motion produced by this event.

Lefkas Island is situated at the northwest tip of the Aegean Arc (Fig 1), one of the most seismic prone areas in Europe, having suffered numerous severe earthquakes in the past [Papazachos and Papazachou, 2003]. Seismic hazard in the area is due to the prominent Cephalonia Transform Fault (CTF, Fig 1), the active boundary between the Aegean and the Apulian plates [Sorel *et al.*, 1976] characterized by dextral strike-slip motion [Kahle *et al.*, 1995] with a slight thrust component [Hatzfeld *et al.*, 1995]. Louvari *et al.* [1999] assumed a division of 40-km long north segment of the CTF, namely the Lefkas Segment (LS) that is capable of hosting an ~6.8 magnitude earthquake according to the empirical relationships provided by Wells and Coppersmith [1994]. This estimate is equivalent to

**CONTACT** Ioannis Kassaras  [kassaras@geol.uoa.gr](mailto:kassaras@geol.uoa.gr)  Laboratory of Seismology, National and Kapodistrian University of Athens, Athens, Greece

Color versions of one or more of the figures in the article can be found online at [www.tandfonline.com/ueqe](http://www.tandfonline.com/ueqe).

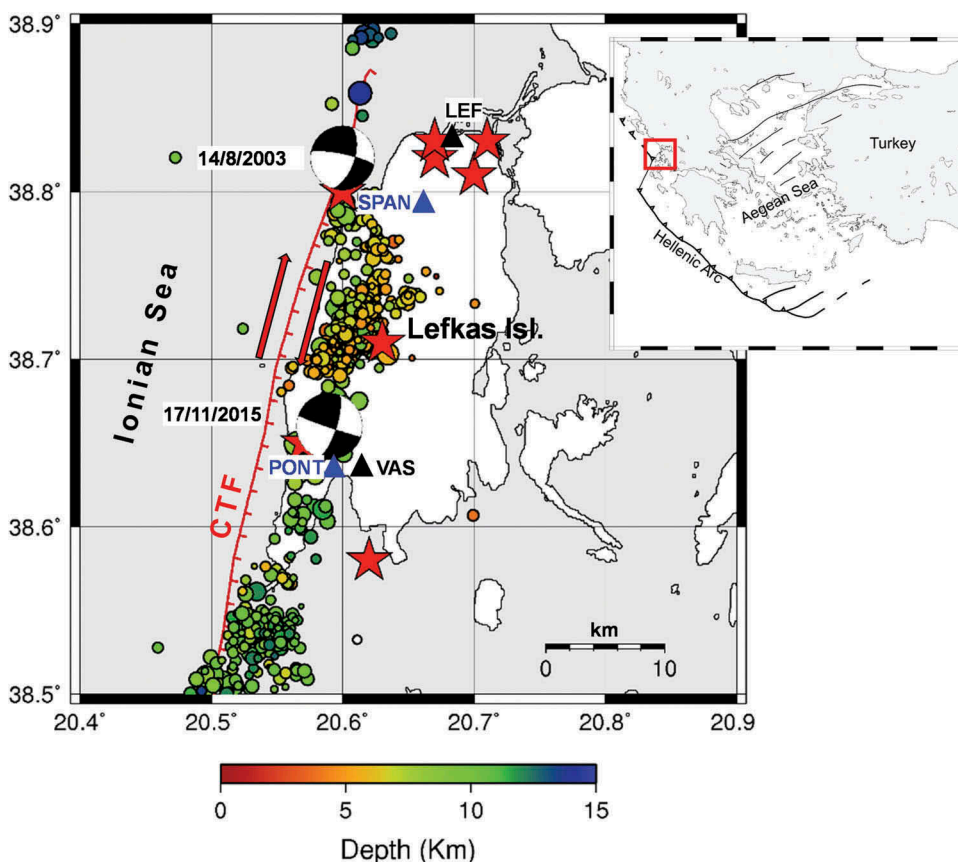


**Figure 1.** Distribution of the relocated 2015 earthquake sequence epicenters [Ganas *et al.*, 2016]. Beach-ball diagrams represent focal mechanisms of the 2003 [Benetatos *et al.*, 2005] and 2015 (GCMT) earthquakes. Red stars denote historical earthquakes with  $M \geq 6$  [Papazachos and Papazachou, 2003]. Solid circles represent instrumental earthquakes with  $M \geq 4$  [Makropoulos *et al.*, 2012]. Black solid triangles indicate the position of permanent accelerometric stations on the island for which recordings of the earthquake are available ([www.itsak.gr](http://www.itsak.gr)). The blue solid triangles denote the position of the NOA GNSS permanent stations (PONT, SPAN). CTF: Cephalonia Transform Fault [Karakonstantis and Papadimitriou, 2010]. LEF indicates also the capital of the Lefkas Island. The red rectangle in the embedded map shows the location of Lefkas within the Greek geotectonic frame.

the magnitude of the largest events that struck Lefkas during the last four centuries [Papazachos and Papazachou, 2003; Stucchi *et al.*, 2013]. Most of the strong earthquakes in the region took place at the north-western part of the island, affecting its capital (Fig 1). Given its seismotectonic setting, Lefkas Island belongs to the highest zone (III) of the current Greek National earthquake design code [EAK-2000, 2003] that predicts a peak ground acceleration  $PGA = 0.36$  g for a return period of 475 years and 10% exceedance probability.

According to the National Observatory of Athens, Institute of Geodynamics the earthquake under study occurred on November 17, 2015, 07:10 GMT at the

southwestern part of Lefkas Island at depth of 11 km (Fig 1) (NOA magnitudes  $M_L = 6.0$ ,  $M_w = 6.4$ , respectively). Two fatalities have been reported, the one due to fall of a stone masonry fence wall and the other due to a rock fall destroying a house, 10 injuries and a median of 20 million USD of loss impact [Daniell *et al.*, 2015]. According to the GCMT Project determination the earthquake occurred on a steep, east dipping dextral strike-slip fault which was also determined from satellite data [Ganas *et al.*, 2016], in agreement with the SSW-NNE oriented CTF. Large co-seismic slip and ground deformation was indicated by GPS and InSAR observations [Ganas *et al.*, 2016; Chousianitis *et al.*, 2016; Melgar *et al.*, 2017; Avallone *et al.*, 2017]. A rich aftershock sequence aligned in a NNE-SSW direction and concentrated at either ends of the activated zone followed the main-shock [Papadimitriou *et al.*, 2017] (Fig 1). The strongest aftershock with  $M_w = 5.1$  occurred 4 km to the SW shortly after the main-shock. A major aftershock with  $M_w = 4.9$  that occurred on November 18, 2015, ~20 km to the north, was intensively felt in the Lefkas capital causing slight structural damage.

The earthquake triggered severe secondary effects at the western part of the island, where Environmental Seismic Intensity [ESI-07, Michetti *et al.*, 2007] was assessed equal to VIII [Papathanassiou *et al.*, 2017]. No primary fault surface ruptures were observed in the field; secondary effect outbreaks were extensive including ground failures, rock falls, landslides, coastal or dock's cracks and soil liquefaction in the southern coastal zone of Vasiliki. Largest effects were observed within the area delineated by the villages of Dragano – Athani – Porto Katsiki and Egremnoi beach and along the road of Tsoukalades – Agios Nikitas related with slope failures, rock falls, rock mass slides, and shallow landslides (Fig 2).

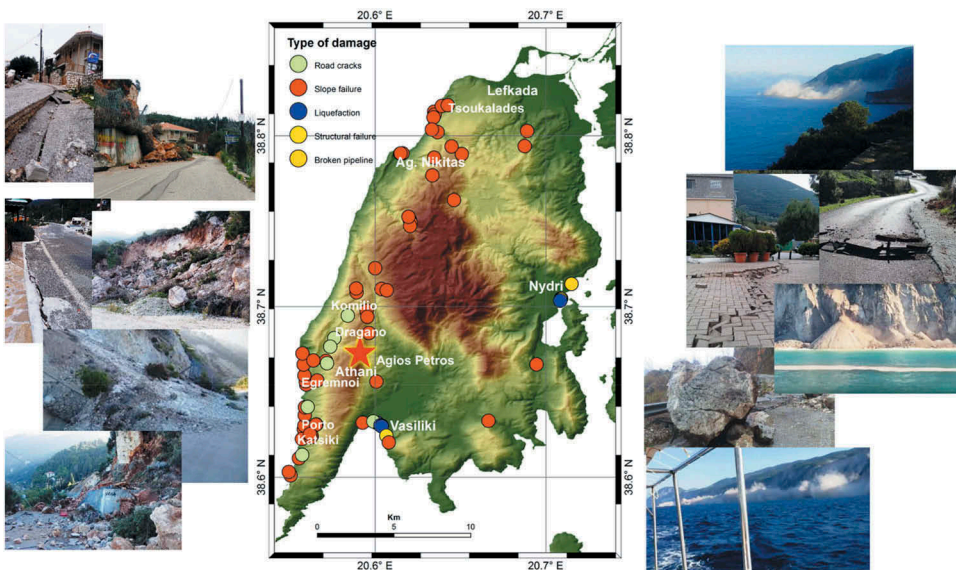


**Figure 2.** Distribution of earthquake-induced effects across the island. The red star denotes the epicenter of the 2015 main-shock. Pictures presenting environmental effects were collected during the *in situ* surveys conducted for the purposes of the current study. Modified after Kazantzidou-Firtinidou *et al.* [2016].

Besides the large size of the earthquake, structural damage was limited within a range of a few km from the epicenter, affecting only a small percentage of the building stock, mainly consisting of non-engineered traditional constructions. These traditional buildings, solely found in Lefkas, have been the subject of intense investigations [e.g. Touliatos and Vintzileou, 2006], and were designated by the European Council Cultural Heritage Unit as earthquake resistant constructions [Kalantoni *et al.*, 2013]. Much of research on this subject has been performed after the Mw = 6.2 earthquake on 14.8.2003 that stroke the northern part of Lefkas, producing extensive but slight-to-moderate damage to its buildings [Karababa and Pomonis, 2011; Kassaras *et al.*, 2014, 2015] and also substantial geotechnical failures [Karakostas *et al.*, 2005; Papathanassiou *et al.*, 2005, 2013], similar to the current event. The earthquake on November 18, 2015 provided fresh observations, motivating our effort to investigate the macroseismic behavior of the local-vernacular constructions situated in the epicentral area. The data on which we rely on are instrumental recordings, empirical vulnerability analysis, structural, and geotechnical damage. Instrumental data comprise acceleration and displacement time-series recorded at permanent stations (Fig 1), whereas results from satellite interferometry were also taken into account. Structural and geotechnical damage data were obtained during three post-seismic field surveys that were carried out by our research group, immediately after the earthquake, between November 19 and 21, 2015, during January 9–12, 2016, and during April 7–10, 2016. The integration of our database has been made possible by the implementation of the comprehensive inspection protocols provided by the local Sector for Earthquake Rehabilitation (SER) which include the age of constructions, the type of their structural system, maintenance state, structural interventions, and type of use, damage description and final usability characterization. This study constitutes a first-order approximation of the 2015 event macroseismic consequences, providing a basis for further analytical research on the expected behavior of structures during forthcoming strong earthquakes.

## 2. Characteristics of strong ground motion

In this section, we investigate characteristics of strong ground motion of the 2015 mainshock that possibly relate to the distribution of macroseismic effects. For this scope, near field recordings of ground acceleration and displacement time series were employed. Strong motion recordings were obtained by the permanent accelerometric stations VAS (Fig 3a,b) and LEF (EPPO-ITSAK) and GNSS PONT and SPAN (GI-NOA stations). VAS experienced the highest peak ground accelerations (PGA) with values up to 0.36, 0.32 and 0.26 g on the NS, EW and vertical components, respectively (Fig 3a). Maximum horizontal PGA of 0.36 g in VAS corresponds to MMI = 8, according to the empirical relation of Tselentis and Danciu [2008]. In PONT the final static deformation amounted up to  $40.3 \pm 0.8$  cm in the S-SW direction with a subsidence of about  $4.3 \pm 1.2$  cm [Avallone *et al.*, 2017].

Source kinematic effects were explored by applying particle motion polarization analysis. The projection of the ground particle motion on the horizontal plane at the accelerometric VAS station (Fig 3b) shows that the maximum horizontal acceleration is polarized into a NW-SE direction, parallel to the T-axis of the focal mechanism ( $341^\circ$  according to the GCMT solution) and along the slope dip of the flanks of the mountainous western part of the island. This



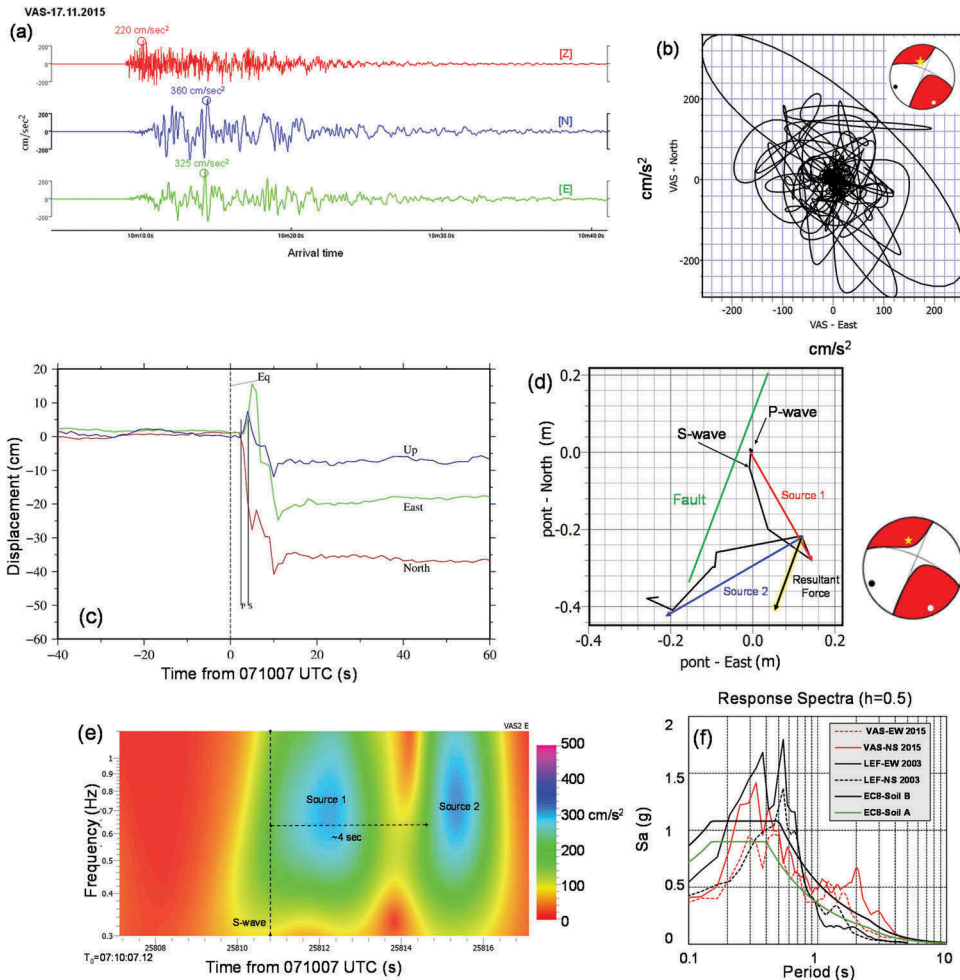


**Figure 3.** Analysis of strong motion recordings: (a) acceleration time-series recording at VAS (see Fig 1); (b) horizontal particle motion at VAS; (c) 5Hz GNSS time-series recording at PONT (see Fig 1); (d) horizontal particle motion diagram of the PONT recording; (e) spectrogram calculated for the E-W VAS acceleration recording; (f) comparison of near-source horizontal pseudo-acceleration spectra of the earthquakes of 2003 and 2015 with design spectra for EC8 soil types A and B. The beach-balls represent the moment tensor solution of the mainshock (NOA); yellow stars denote the projection of VAS, PONT on the focal sphere; black and white dots are the projection of P- and T-axis, respectively.

attribute is not observed in LEF which is located further, about 20 km to the north of the hypocenter. Panels c and d of Fig 3 present the analysis of 3-component displacement time series recorded at the GNSS permanent PONT station, and the horizontal particle motion polarization, respectively. Fig 3c suggests that rupture static effects are distributed in two distinct pulses, collinear with the T- and P-axes of both the inferred focal mechanism of the earthquake, and the regional stress field [Kassaras *et al.*, 2016]. The arrival of the first pulse matches the S-wave arrival, occurring 4 s after the origin time. The second pulse arrives 4 s later. The resultant of two exerted forces from the two sources is collinear with the horizontal displacement vector of the coseismic deformation, measured equal to 40 cm toward SSW [Ganas *et al.*, 2016]. This pattern

is similar with dynamic displacements deduced for an  $M_w = 6.9$  strike-slip earthquake occurred in 2014 in north Aegean [Saltogianni *et al.*, 2016]. It is worth noting that SPAN, located north of the mainshock, did not exhibit a relevant configuration.

Frequency-Time Analysis (FTA) performed for E-W VAS recording (Fig 3e) indicates the occurrence of two discrete sources. Two main contributions are displayed; a small one 4 s after the origin time (S-wave arrival in VAS, PONT) and another one 4 s later (panels c and e of Fig 3). A similar configuration was indicated from the analysis of regional [Zahradník and Sokos, 2015; Sokos *et al.*, 2016] and teleseismic [Chousianitis *et al.*, 2016] recordings.

Ground motion parameters were computed in VAS using SeisMOSignal [SeisMOSoft, 2016] (Table 1): PGA reached but did not exceed the maximum expected value of effective acceleration 0.36 g of the seismic code. The largest ground motion values are observed in the N-S component, sub-parallel direction to the causative fault. Horizontal Arias intensity, a ground motion parameter considered representative of the earthquake impact on slope stability [Arias, 1990] reached 1.5 (E-W) and 2.6 (N-S) m/s exceeding values predicted for the Greek territory [Chousianitis *et al.*, 2014] at a hypocentral distance  $r = 12$  km. Significant durations for the 5–75% of Arias intensity, i.e. the shortest duration over which 70% Arias intensity accumulates [Trifunac and Westermo, 1982], exceed values predicted by empirical relations deduced for active tectonic regions [e.g. Bommer *et al.*, 2009; Afshari and Stewart, 2016]. The respective value of significant duration for 5–95% of Arias intensity is about 15s. Such a value, according to Bommer *et al.* [2004] may lead to an increased structural strength degradation of the building with respect to its initial state.

Predominant period of the peak horizontal acceleration at VAS (0.3 and 0.5 s) (Table 1) lies beyond the elastic response of low-rise constructions (max 2–3 story) which are mostly found in the epicentral area, having a different elastic response, below 0.2 s [Karakostas *et al.*, 2005]. The predominant period of 0.1 s of the vertical component matches the response of these stiff constructions, implying that this component has possibly played a role to the damage, besides its lower value with respect to the horizontal ones. Spectral acceleration ( $S_a$ ) according to the 2003 and 2015 earthquake recordings at LEF and VAS, respectively, is presented in Fig 3f as an additional explanatory variable, in comparison to the elastic design spectra of the EC8 [Cen, 2004] provisions for soil types A and B. The spectral amplitudes of the current quake present one cycle of strong shaking of 1.4 g at 0.33 s, with respect to the bimodal response of the 2003 event ( $\sim 1.7$  g at 0.4 s and  $\sim 1.8$  g at 0.55 s). Spectral acceleration of the current event exceeds the provisions of the design spectra but the period of the peak value (0.35 s) explains the limited severity of structural damage in the epicentral area, as it lies away from the horizontal response of the constructions [ $<0.2$  s; Karakostas *et al.*, 2005].

**Table 1.** Strong ground motion parameters at VAS.

Parameter	Component		
	Z	E-W	N-S
Max. Acceleration ( $\text{cm/s}^2$ )	220	325	360
Max. Velocity ( $\text{cm/s}$ )	21.4	34.7	54.2
Max. Displacement ( $\text{cm}$ )	6.3	15.6	20.1
Arias Intensity: ( $\text{m/s}$ )	1.0	1.5	2.6
Predominant Period (s)	0.1	0.5	0.3
Significant Duration of 5–75% of Arias Intensity (s)	6.9	8.0	7.3
Significant Duration of 5–95% of Arias Intensity (s)	12.4	15.4	14.0

### 3. Exposure model and empirical vulnerability

A key factor for explaining seismic damage is the vulnerability estimate of the buildings. In this section, we present the main characteristics and the distribution of 6 building typologies found in Lefkas after post-seismic field surveys carried out by our research group. These typologies consist of modern reinforced concrete (RC) and older non-engineered buildings constructed using various traditional practices. According to the latest census data [National Statistical Service of Greece (NSSG), 2011], the building stock of the island comprises 54% concrete, 30% stone masonry, 6% timber, 6% brick masonry and 3% other materials in a total of 15,700 buildings. Fig 4 presents examples of the Lefkas buildings typologies, as initially recognized by Karababa and Pomonis [2011] and Table 2 summarizes the main attributes applied per building typology for the EMS-98 vulnerability classification, discussed in the next paragraphs. Fig 4 presents the distribution of the building typologies throughout the island.

#### 3.1. RC Buildings

The RC structural frame system was introduced in the capital of Lefkas (see Fig 1) after the strong earthquakes of 1948 (M6.4–6.5) and later on it was expanded to the rural areas to the south. Its use was generalized after 1960's, but neither engineering supervision nor design plans were always accomplished. Their vulnerability, after EMS-98 is medium to low (C class or higher) depending on the construction era, which determines the design code in force. Over 60% of the RC building stock has been erected before 1995, when the modern seismic code became compulsory, with respect to the one issued in 1959, been the first code to provide seismic design guidelines and construction detailing in Greece. It is important, though, that, given the seismic activity of the area, the quality of workmanship has been proven to be in general higher than seen in other regions of Greece [Karakostas *et al.*, 2005].



**Figure 4.** Examples of the Lefkas buildings typologies. Photos taken by our group in 2015–2016 and Kalantoni [2016].



**Table 2.** Structural typologies of Lefkas and EMS-98 vulnerability class assignment [Karababa and Pomonis, 2011; Kassaras *et al.*, 2014]. Asterisks (\*) denote the new elements highlighted in this work. ERD: Earthquake Resistant Design (following seismic code provisions).

Typology	Description	EMS-98 Vulnerability class (most probable)	Percentage over total stock (%)
<i>Reinforced concrete frame (RC)</i>	Without ERD (<1960)	C	2.5%
	With moderate ERD (1960–1994)	D	20%
	With high ERD (>1994)	E	22%
<i>Load-bearing stone masonry (LBSM)</i>	With thick walls, flexible timber diaphragms, mainly built prior to 1960	A or B depending on the level of maintenance	30%
<i>Timber frame structures (TF)</i>	With locally supplied timber, flexible timber diaphragms, mainly built in 1946–1960	B to D depending on the level of maintenance	4%
<i>Dual load-bearing stone masonry and timber frame structures (LBSM-TF)</i>	Two-story. Dual system of load-bearing stone walls in the ground floor, timber columns supporting the upper story ( <i>pontelo</i> ). The upper story is constructed with infilled timber frames. Most were built prior to the end of the eighteenth century	B to D depending on the level of maintenance	10%
<i>Mixed load-bearing masonry &amp; Reinforced concrete structures (LBSM-RC)</i>	Mixed system of load-bearing stone or brick walls confined with reinforced concrete vertical and horizontal elements, timber joists or cast in-situ RC slabs, mainly constructed in 1960–1985	B to D* depending on the construction period, level of maintenance, material of confinement elements	10%
<i>Load-bearing stone masonry with internal load carrying timber columns (LBSM-TC)</i>	One or two-story with stone masonry load-bearing walls, secondary internal structural system with timber columns <i>pontelo</i> supporting the floor and roof	B to C*	2%

### 3.2. Traditional buildings

Traditional buildings in Lefkas are in general classified as (a) Timber-Frame structures (TF), (b) Load-Bearing Stone Masonry structures (LBSM) with its LBSM-RC (LBSM with RC lintel) counterparts, (c) Dual LBSM (LBSM-TF and LBSM-TC), having a secondary timber system known as *pontelo*. These buildings, unique within the Greek territory, have attracted the interest of structural engineers, architects and historians aiming at thoroughly investigate their historical evolution and seismic performance [Papadatou-Giannopoulou, 1999, 2014; Touliaos and Vintzileou, 2006; Vintzileou *et al.*, 2007a, 2007b; among others]. Historical evidence [Papadatou-Giannopoulou, 1999] shows that economic restrictions of the population and frequent catastrophic earthquakes imposed the use of indigenous construction materials (timber, rubble stones and mortars), combined in a unique traditional technique. Records on the effects of strong earthquakes of the Ionian Islands available since 1469 demonstrate for the first time the exceptional seismic behavior of the *pontelo* buildings of Lefkas after a destructive earthquake occurred on October 2, 1613 [Papadatou-Giannopoulou, 1999]. It is worth noticing that during the Venetian era (1684–1810) a detailed damage dataset per building typology was kept, presently available in the Municipality Archives [Tonna, 2014; Tonna and Chesi, 2016]. The severe impact of the catastrophic 1825 earthquake, which occurred during the British era (1810–1864), led the administration to issue a Construction Code in 1827, based on a robust analysis of the most affected structures and materials, having realized the enhanced performance of this unique construction system [Tonna and Chesi, 2015]. The period between 1825 and 1920 is

characterized by a large construction activity and the use of this construction type has been expanded throughout the island. The different typologies of traditional buildings are described below with extended reference to the *pontelo* technique. The traditional buildings of the Lefkas municipality have been acknowledged by the Greek government as of “Special Architectural or Historic Interest” since 1982, and any man induced deterioration of their characteristics is not allowed [government paper sheet B103, 1982].

### 3.2.1. Timber Frame structures (TF)

This typology is present mainly in the capital of Lefkas Island and the seafront regions (Fig 4), where the local population possessed the craft of the wooden shipbuilding, on which the house construction is assumed to be based [Papadatou-Giannopoulou, 2014]. The timber in use was mainly wild wood (oak, fir, and cypress), thanks to the large dimensions and its enhanced bearing capacities, while flexible olive tree wood or roots were used for the corners. The trunks were immersed into the mud of the lagoon in eastern Lefkas, a controversial technique applied for sealing the wood prior to the application, to protect it from deterioration. Often the wood was also coated with tar. The external sheathing was initially wooden as well but, due to the wet climate, it was later replaced by smooth or corrugated iron plates, which lead to the architectural degeneration of the typology [Papadatou-Giannopoulou, 1999].

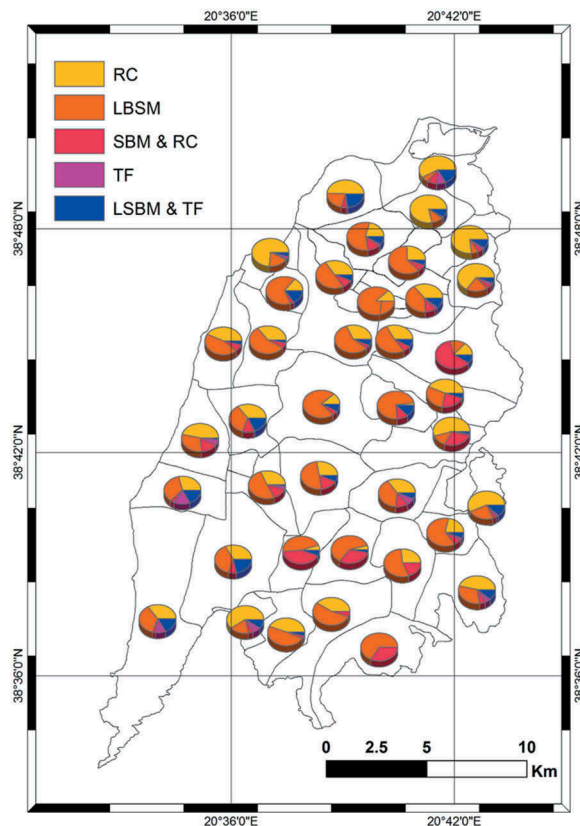


**Figure 5.** Distribution of building typologies across Lefkas [data from Karababa and Pomonis, 2011].

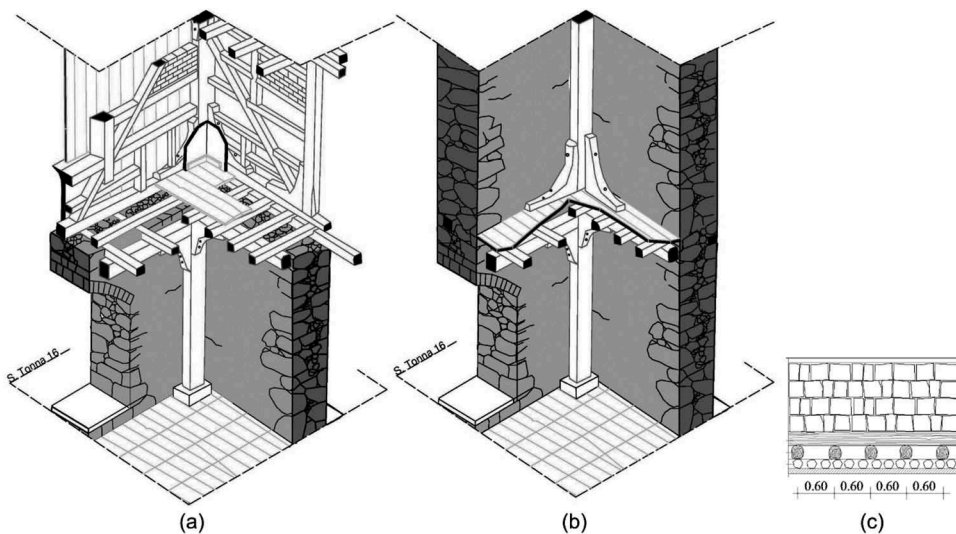


**Figure 6.** Exhibits of (a) the LBSM-TF system, (b) the LBSM-TC system [Tonna, 2016; for the purpose of this study], and (c) their foundation system comprising three layers, round stones, wooden grid and stones with mortar [after Papadatou-Giannopoulou, 2014].

The timber frame is exceptionally well modulated by a proper horizontal and vertical grid of studs and girders, diagonal stiffening rods and corner reinforcement, similar to the upper floor of the exhibit shown in Fig 6a. The vertical components can have a cross section up to 22 cm. The interbonding system incorporates timber nails and dowels, taking advantage of their ductility and tensile resistance. They are light constructions generally corresponding to small, low, and regular structures, well adaptable to the seismic excitations. Hence, their vulnerability, following EMS-98 guidelines, ranges between B and D depending on their maintenance state [Kalantoni, 2016].

### 3.2.2. Load-Bearing Stone Masonry Structures (LBSM)

Load-Bearing Stone Masonry Buildings in Lefkas (LBSM) are one or two story buildings having walls of thickness between 0.6 and 0.7 m (in two wythes) and height up to 3 m. The internal wythe is usually composed by irregular size and shape rubble stones [Karababa and Pomonis, 2011]. The mortar varies according to the period of construction. In the early construction period, clay-lime material was used whereas later it was replaced by cement mortar. Analysis on mortar specimens [Tonna *et al.*, 2014] evidenced high-quality material suitable to provide enhanced hydraulic properties to the mortar. The floors are wooden planks fastened on timber beams and the roofs are made of timber trusses covered with clay tiles [Kassaras *et al.*, 2014]. Vertical steel “blades” or “anchors” of 1 m length and 12–15 cm width, anchored into the wooden floor are often embedded in the mortar at both sides of the walls to provide a coupled performance to the walls-floor structure [Malakasis, 2000]. This typology is found throughout the island and is predominant at the inland villages (Fig 5). Since they consist non-ductile, loosely bonded constructions, with several modes of failure,

highest vulnerability was attributed to this typology, between A and B, depending on the maintenance state.

### 3.2.3. Mixed Load-Bearing Masonry & RC Structures (LBSM-RC)

LBSM-RC buildings employ concrete ring beams with light reinforcement, or cement mortar bands at the lintels or roof level. The roofs are timber trusses similar to the LBSM typology. These strengthening elements significantly enhance the structural integrity contributing to the box behavior of these buildings. According to cross-referenced testimonies of living memories collected during our surveys, this configuration, called “nucleus”, has been adopted after the disastrous earthquakes of the mid-twentieth century (1948 and 1953). Better confinement of the masonry of these buildings leads to lower vulnerability, assessed B-D herein, according to the construction period, materials quality, reinforcement of the constituent elements and the state of health.

### 3.2.4. Dual LBSM (Pontelo)

This study highlights in particular LBSM constructions involving a secondary timber load-bearing system, so-called *pontelo*, being the main element of the unique earthquake resistant design traditional technique of Lefkas (Fig 6). This structural system, dating back at least to the eighteenth century [Papadatou-Giannopoulou, 1999] represents ~10% of the building stock of the island and it has been widely acknowledged for its seismic performance [Karakostas *et al.*, 2005; Vintzileou *et al.*, 2007a; Karababa and Pomonis, 2011; Tonna, 2014]. According to Papadatou-Giannopoulou [1999], the concept of utilizing timber elements for supporting upper-floor constructions originates in the ancient era. The secondary *pontelo* load-bearing system is found in two variations, LSBM-TF (Fig 6a) and LSBM-TC (Fig 6b). Both variations exhibit a sophisticated foundation system first with a layer of pebble stones, followed by a grid of trunks, which provided deformability to the structure, and topped with several layers of rubble stones applied in an attempt of traditional consolidation of the loose soil which is predominant in Lefkas town and in the eastern lagoon [Papadatou-Giannopoulou, 2014] (Fig 6c). In the following sub-sections, each building variation is described in more detail.

### 3.2.5. LBSM-TF

This construction type is found throughout the island and represents a historical earthquake-resistant structure, uniquely encountered in Lefkas [Vintzileou *et al.*, 2007a, 2007b; Papadatou-Giannopoulou, 1999, 2014]. These are two or three-story buildings that consist of a stone masonry ground floor and one or two timber frame upper story(s). The external bearing walls consist of two well-tied wythes connected by diatones or semi-diatones, linked together by a cohesive clay-lime mortar. In the interstices, timber wedges are applied and the angled masonry walls are well organized so as to oppose the tendency of the perimeter angular joints to fail out-of-plane. The floors and roofs are hyper-statically supported [Vintzileou *et al.*, 2007a], with the *pontelo* secondary structural system, running parallel to the masonry structure at the ground floor. The latter is partly charged by the flexible timber first floor (Fig 6a). In case of partial or total collapse of the masonry walls, the *pontelo* system provides support against vertical loads through its short cantilevers, and accounts for the

security of the occupants. A conceptual favorable property of the dual system is the differential eigenmode of the constituents leading to a quasi-widening of the elastic response spectrum for the whole construction.

The upper infilled timber frame absorbs effectively the lateral loads thanks to the orthogonal and diagonal timber elements and the angular reinforcement of the frame, allowing for a stiff join of all elements and hence a lateral stability and stiffness (Fig 6a). Different configurations of the timber trusses have been found in Lefkas, Vasiliki and the inland villages. The infill material is of much lower mass (and consequently lower elastic modulus) than the bearing masonry of the ground floor. In the inland, no protective material against erosion is present at the external part of the walls (i.e. metal panels), therefore vulnerability is increased by the climate conditions. The partition walls are light aseismic constructions comprising timber frames filled with wattle. The flexible low mass second story provides relief from high inertia that stone walls would experience and lateral deformability to the structure. We conclude a vulnerability class better than B for these buildings in agreement with Kassaras *et al.* [2014].

### 3.2.6. LBSM-TC

The constituent systems of this typology are 1–2 story stone masonry shear walls of 60–70 cm thickness and interior vertical load bearing timber columns (TC) that extend to the ground, while joists and trusses constitute the floor and roof (Fig 6b). In case of failure of the walls, the secondary timber frame system provides alternative transfer path for the vertical loads of the timber floors, similar to the LBSM-TF typology described above. According to cross-referenced local testimonies, it is considered likely that the traces of this structural typology date roughly before the end of nineteenth century. Further, it is not clear whether the timber column elements were erected concurrently with the stone masonry construction, or they were added at a later stage after acknowledging their seismic performance.

The structural performance of LBSM-TC is not different from a typical LBSM structure, given that the partial independence of the flexible wooden diaphragm, of low mass, makes small difference to the lateral performance of the structure. Due to the absence of rigid linking elements between the walls, according to Makarios and Demosthenous [2008], local modes of out-of-plane oscillation can be induced. Hence, despite the “life safety” function provided by the internal timber frame, thanks to which complete collapse is often avoided, the seismic vulnerability of the bearing walls is considered of the same order or slightly lower (B-C). Such buildings are mainly located at the villages of the internal part of the island.

## 4. Spatial Distribution of Structural Damage

In this section, we present comprehensive damage characterization provided by the local SER, obtained after two official post-earthquake damage inspections performed by engineers (Table A1 in Appendix A). During the first “rapid” inspection 1500 buildings were checked under request of their owners; in total, about 700 buildings were found affected after a second order survey, the damage of each has been registered in official protocols. The damage state for each building was concluded by the experts following the EPPO guidelines [Anagnostopoulos and Moretti, 2008] that define the main characterization



**Table 3.** Post-seismic usability and damage classification [Anagnostopoulos and Moretti, 2008] with respect to the discrete EMS-98 damage grades.

Usability characterization	Description	EMS-98 Damage Grade
<i>Safe for Use "Green"</i>	Buildings with no reduction of their seismic capacity	DS0 – None DS1 – Slight
<i>Unsafe for Use "Yellow"</i>	Buildings with reduced seismic capacity, not to the extent of being in danger of sudden collapse. In need of repair before re-occupation.	DS2 – Moderate DS3 – Heavy
<i>Dangerous for Use "Red"</i>	Buildings with prohibited approach, seismic capacity greatly reduced, prone to collapse. Decision on possible repair or demolition is indispensable.	DS4 – Very heavy/Severe

criteria as the safety of the users, based on the estimate of the post-seismic bearing capacity of the constructions and the presence of some additional hazardous conditions (Table 3).

Following these guidelines, inspected buildings are registered as following: “Green – Safe for Use”, “Yellow – Unsafe for Use” and “Red – Dangerous for Use”. The SER post-seismic inspections were evaluated by our observations and concluded to 207 “Green”, 444 “Yellow” and 51 “Red” buildings. It is worth mentioning that in Greece, damage inspection is typically undertaken upon the building owner request. For the same reason, unoccupied but possibly affected buildings have most probably not been investigated,

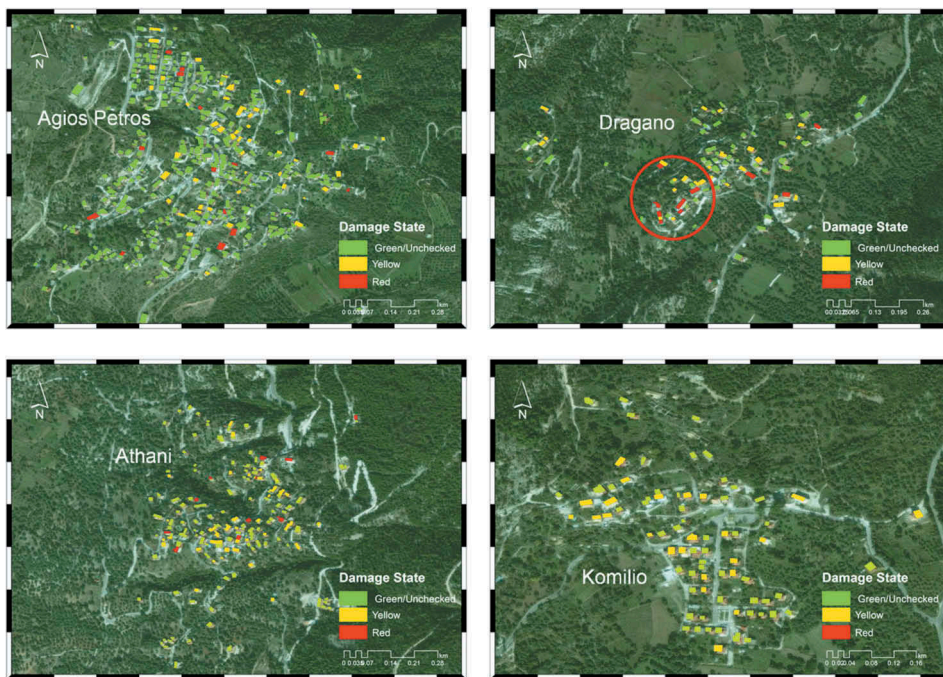


**Figure 7.** Maps showing the damage distribution in the epicentral area by combining satellite imagery, comprehensive SER protocols and data from an *in situ* surveillance. The red circle in Dragano indicates location of Fig 8.

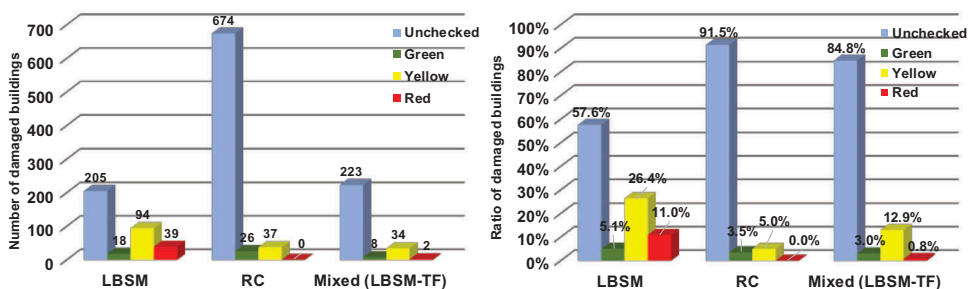


**Figure 8.** Field photographs (July 2016) showing structural damage imposed by an earthquake-induced landslide at Dragano.

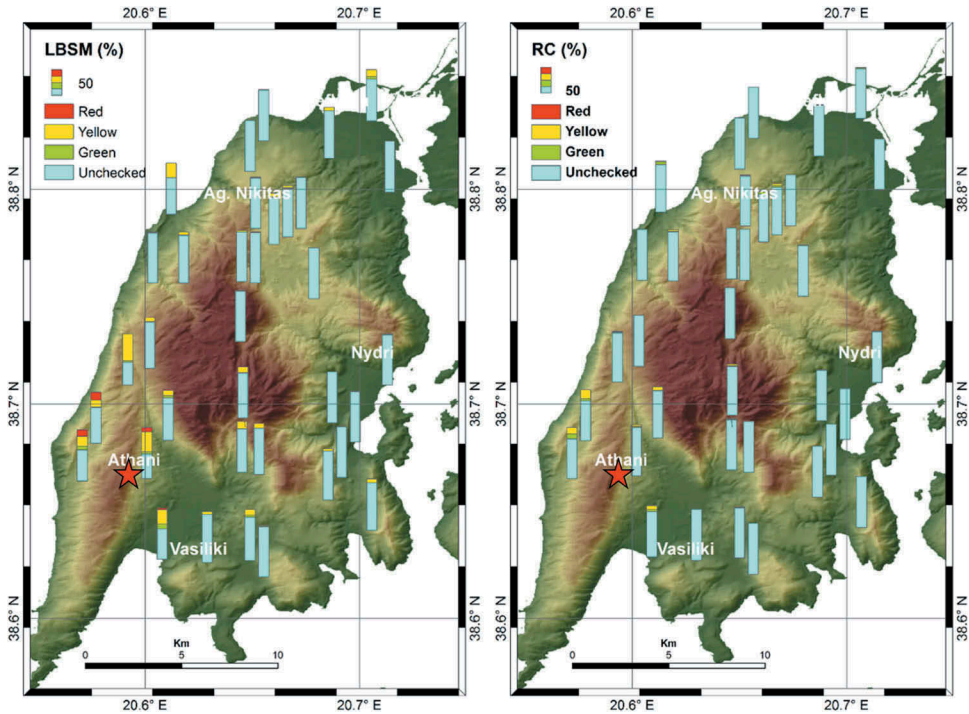
especially in the non-epicentral area. “Green” buildings according to the descriptions of the SER dataset may present none or slight damage.

Fig 7 shows the spatial distribution of damage at the most affected villages of Komilio, Dragano, Athani and Agios Petros (see Fig 2 for location), in terms of “Green”, “Yellow”, “Red” color coding, after SER. To produce these maps, given the lack of vector data in the area, satellite imagery was employed and processed to acquire the building footprints in the epicentral area. Damage characterization was then placed on the footprints after identifying the locations of buildings in the SER protocols by an additional in-situ survey conducted in April 2016. It is worth noting the case of Dragano where damage related to out-of-plane failure of the bearing walls (Fig 8) reported at the western part of the village (circled in red in Fig 7) is thought to be caused by an earthquake-induced slope failure.

In the most affected area of the abovementioned districts (Agios Petros, Dragano, Athani, Komilio), the following data is registered for the total RC buildings, load bearing stone masonry buildings (LBSM) and mixed ones: [LBSM: 18 or 5.1% “Green”, 94 or 26.4% “Yellow”, 39 or 11% “Red”], [RC: 26 or 3.5% “Green”, 37 or 5% “Yellow”], [Mixed: 8 or 3.0% “Green”, 34 or 12.9% “Yellow”, 2 or 0.8% “Red”] (Fig 9). The total number of buildings per district is obtained from the 2011 census [National Statistical Service of Greece {NSSG}, 2011]. Site investigation has revealed that the “mixed” buildings refer mainly to the LBSM-TF ones, for which a double system is apparent, whereas the “stone”



**Figure 9.** Absolute number of usability characterization (color tag) per building typology (left) and percentage of characterized buildings (right) for the four most affected districts.



**Figure 10.** Percentage distribution of usability characterization (tag) per location, and bearing material according to SER data for LBSM and RC typology. Red star denotes the epicenter of the current earthquake. The number and percent of damaged buildings is given in [Table A1](#) (Appendix A).

ones include both the LBSM and LBSM-TC. Since the total number of “mixed” buildings is not explicitly provided by the most recent 2011 census data, the total number of their stock is adopted from Karababa and Pomonis [2011], assuming negligible change for the multitude of this typology thereafter. In this study, it was assumed that “unchecked” buildings present no apparent damage, except for cases that our field surveillance indicated the opposite. In overall, the usability characterization of the buildings throughout the island has revealed 95 or 1.1% “Yellow” RC buildings, 285 or 6.4% “Yellow” and 45 or 1.0% “Red” LBSM buildings and 59 or 3.9% “Yellow” and 6 or 0.4% “Red” of the mixed typology. As it can be seen from [Table A1](#) (Appendix A) and [Fig 10](#), LBSM was the most damaged structural typology in the epicentral area.

[Fig 11](#) presents the reported damage distribution of the 2003 and 2015 earthquake of all building typologies with respect to the epicentral distance. The figures show that damage decays with distance, as expected and this is more explicit in 2015 earthquake. For the case of the 2003 event ([Fig 11a](#)), higher discrepancies are observed, given that damage was distributed in a wider radius, whereas in 2015, the relative damage per district’s building stock decays significantly within a small epicentral distance ([Fig 11b](#)). When comparing with the total damage throughout the island, the 14% of the total building stock have been characterized as unsafe or dangerous due to the 2003 earthquake versus 3% due to the 2015 one. The larger amount of total damage during the 2003 earthquake can be first explained by the fact that structural damage was registered at some level almost



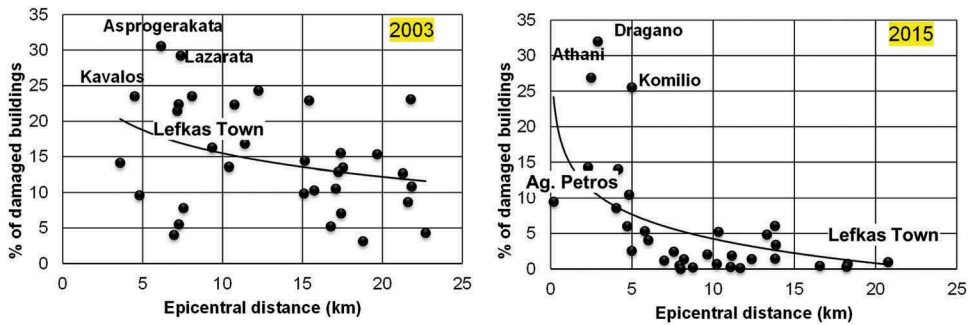


**Figure 11.** Relative number of damaged buildings per total building stock of every checked urban district, with respect to the epicentral distance for the 2003 (left) and the 2015 (right) earthquake. Black solid lines represent polynomial fit to the individual data points that correspond to cumulative observed damage per district (solid circles). Details for the 2003 event can be found in Karababa & Pomonis (2010) and for 2015 event in Table A1 (Appendix A).

throughout the entire island (Fig 11, Fig 16), but also by the fact that the event affected the densely populated northern part of the island (incl. the capital town) with a much more important exposed building stock. The damage configuration of the two earthquakes can be explained by the rupture kinematics of the two earthquakes: during the 2003 event, rupture initiated in the north and propagated to the south reaching the northern coast of Cephalonia Island [Benetatos *et al.*, 2007], thus affecting the whole Lefkas island; during the 2015 earthquake, the maximum slip was concentrated south of the epicenter [Melgar *et al.*, 2017], affecting mainly the southern part of the island, which is sparsely inhabited.

## 5. Damage per Structural Typology

In this section, we quote the damage characteristics per building typology as it has been registered through our *in situ* post-seismic surveillance and the SER protocol entries. In overall, limited damage has been registered to all building typologies. The satisfactory seismic performance can be attributed to both the meticulous construction as well as the dynamic characteristics of the event itself. As the elastic spectra of Fig 3d indicate, the spectral acceleration and ductility demand were more important at



**Figure 12.** Damaged RC buildings in Athani: (a-b) Damage to columns and beam column joints at RC buildings; (c) Large cracks at infill panels.

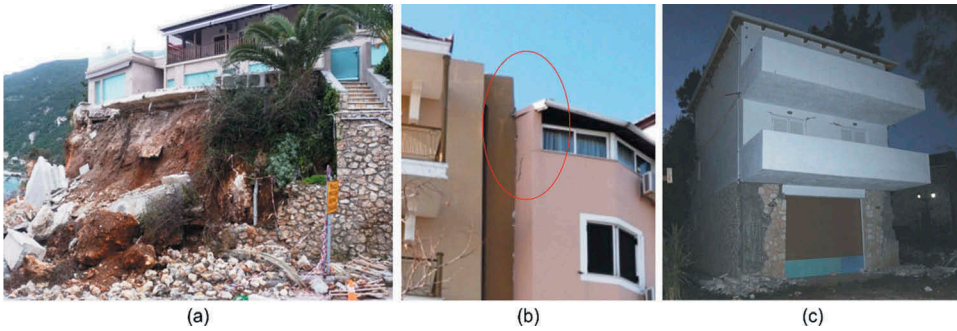


**Figure 13.** The crack pattern surveyed for the traditional LBSM-TF typology: (a) An abandoned house in Lefkas town with in-plane diagonal shear cracking; (b) Building in Agios Petros with wall angle detachment due to ground subsidence; (c) “Red” tagged building in Athani with timber frame vertical deviation.



**Figure 13.** (Continued).



**Figure 14.** (a) LBSM “Yellow” tagged building in Agios Petros; (b) Damage of a single floor LBSM-TC in Athani; (c) LBSM-RC in Kalamitsi remained intact after the earthquake.

periods higher of the low fundamental periods ( $T < 0.2$  s) of typical low rise local structures [Karakostas *et al.*, 2005]. Taller buildings are RC structures, built with some earthquake resistant design provisions, possessing additional strength and ductility reserves and are few in number in the epicentral region.





**Figure 15.** (a) Red tagged LBSM-TC building in Dragano with successful performance of TC frame (b) Collapsed Agia Paraskevi church in Athani; (c) Collapsed kiosk near Athani.

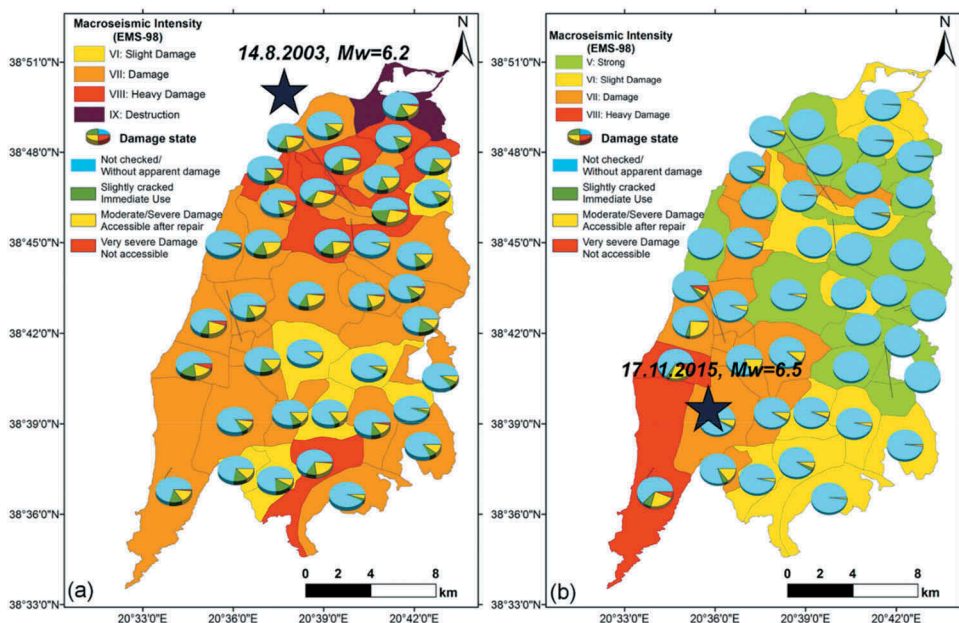


**Figure 16.** Composite maps showing the spatial EMS-98 macroseismic intensity and structural damage state estimate per administrative sector of the island for: (a) the 2003 earthquake using census data [NSSG, 2001] and data of Karababa and Pomonis [2011], epicenter from [Ilieva *et al.*, 2016], (b) the 2015 earthquake, based on the analysis of the present study, and census data [National Statistical Service of Greece (NSSG), 2011]. Pies indicate post-seismic usability characterization of buildings over the total building stock per sector.

### 5.1. Reinforced Concrete Buildings (RC)

In total, 95 of these buildings have been registered “Yellow”, mainly concentrated in the southwestern peninsula at the villages of Dragano, Athani, Komilio, and Agios Petros (Fig 10 right). These are RC infilled frame low-rise buildings with up to two story, constructed before 1995, according to the early ERD provisions of the first Greek Seismic Design Code issued in 1959 and its enhancements issued in 1985. In this regard, low base shear seismic design coefficient was uniformly applied according to the allowable-stress design method, which for

the case of Lefkas on medium soil is  $\epsilon = 0.12$ . This coefficient is equivalent to  $\epsilon' = 0.21$  for the ultimate strength design [Karakostas *et al.*, 2005]. Typically, RC buildings in the epicentral area of the 2015 event are of low-to medium height (max. three stories), with relatively small mass and fundamental period [ $T < 0.15 \div 0.20$ sec, Karakostas *et al.*, 2005]. It is obvious from Fig 3f that such buildings were not heavily stressed, due to the particular shape of the response spectrum of the mainshock which reaches its peak beyond 0.3 s. The ductility demands imposed by this particular earthquake, even on pre-1995 RC buildings in this period range were not too high (i.e. for  $0 < T < 0.20$  s and respective  $0.33 g < S_a < 0.84 g$  for the medium soil types of the area, ductility demands with respect to the design values are in the range of  $1.6 < D < 4.0$ ), thus explaining the limited damage observed.

Arbitrary/erroneous interventions observed on site, i.e. improper structural detailing, spacing among stirrups, improper anchorage, use of smooth rebars, materials of questionable quality, and degradation due to aging, were factors that increased the susceptibility of the buildings to local or overall damage but were only identified in limited cases in the area considering the locals' seismic experience. Moreover, the overstrength offered by the energy dissipation of the infill walls and/or the good quality of materials and workmanship were proven capable to enhance the buildings' performance, contrary to their seismic behavior assessed by numerical modeling [Karakostas *et al.*, 2005], for moderate eccentricity. Hence, most commonly the damage was mainly observed at the non-structural elements of the RC buildings of any erection period.

The structural damage described in SER documents for "Yellow" buildings and observed on site were cracks in RC elements (beams, columns, joints) at different extent, spalling of concrete cover and buckling of rebars for some limited cases (Fig 12a, b). The most common failure is related to delamination and diagonal cracking of the infill panels (Fig 12c). In several cases, buildings have been characterized "Yellow" due to local soil instability and foundations compliance. Hairline cracks at infill walls or at the plaster of structural elements and limited dislocation of tiles led to "Green" characterization. Non-structural damage, such as cracks in partition walls, fall of brittle cladding and mortar (Fig 13c), account for Grade 2 (moderate damage) and "Unsafe for use" characterization.

Other source of damage was the static ground deformation, which has not been possible to be assimilated by separate footings, especially of the older buildings. As far as the response of RC buildings located at larger epicentral distances is concerned, failures were mostly generated by earthquake secondary effects, such as landslide and slope failure, ground subsidence and mutual pounding between adjacent buildings due to insufficient or lack of seismic joints (Fig 13a,b).

## 5.2. Traditional Buildings

### 5.2.1. Timber Frame Structures (TF)

As mentioned before, the majority of TF buildings are mainly found in the regions of Lefkas capital and the eastern part of the island that suffered slightest intensity of the order of V and sporadically in Vasiliki, where earthquake effects were minor (Fig 16). These buildings have not been majorly affected by the earthquake, with the exception of few abandoned ones with a very poor state of maintenance. Regular shape, light mass and structural elasticity have contributed to a favorable seismic behavior.

### 5.2.2. Mixed Dual Load-Bearing Stone Masonry and Timber Frame Structures (LBSM-TF)

Several “Yellow” tagged structures of this typology have been registered, mainly at the epicentral area. Only nine LBSM-TF buildings have been characterized as “Red”, having suffered vertical deviation of the timber framework and extensive cracking of the shear stone masonry walls. Damage registration performed for several cases at various locations showed different structural behavior. This may be due to the state of preservation and the characteristics of the structural components, depending on the period of construction. Damage was mainly concentrated at the stiff ground floor by diagonal shear cracks initiating at the openings (doors, windows) (Fig 13a), whereas the infill material of the upper timber frame structure was cracked and at times dismantled. Interestingly, non-linear dynamic analysis of a LBSM-TF structure indicates high tensile stresses concentrated specifically at these failed zones [Karakostas *et al.*, 2005].

For the herein purposes, we performed a cross-check inspection of several buildings in the capital of Lefkas, considering damage observations after the 2003 earthquake [Kalantoni *et al.*, 2013; Tonna, 2014; Tonna and Chesi, 2016]. For some cases, previously damaged but unrepaired structures presented worsening of their state jeopardizing their integrity and also safety of the surrounding area (Fig 14a). No essential structure-related collapse mechanisms other than vulnerability increment by accumulated seismic strain have been detected. Coseismic ground deformation is found to affect the stiff ground floor producing severe cracking of the masonry (Fig 13b) and timber frame walls. Buildings with severely damaged stone masonry walls and/or large lateral displacement of the timber upper story did not collapse (Fig 13c), manifesting the satisfactory seismic performance and integrity of the secondary *pontelo* load-bearing system.

### 5.2.3. Load-Bearing Stone Masonry Buildings (LBSM, LBSM-TC, LBSM-RC)

Although 65% of “Yellow” and 88% of “Red” tagged buildings, correspond to the LBSM typology, their seismic response is considered satisfactory, given their multitude across the epicentral area (Fig 5, Fig 10 left). All LBSM buildings variations presented a similar behavior/failure pattern regarding the primary stone masonry load bearing system, i.e. separation of walls at intersections, cracking and tilting of wall panels due to out-of-plane mechanisms, diagonal in-plane cracks initiating from weak areas, delamination of wall wythes loosely interlocked (Fig 14a). Dislocation and fall of roof tiles has been often observed.

The *pontelo* secondary timber load-bearing system of the LBSM-TC buildings, partially discharged the bearing walls and prevented the push over of the masonry walls imposed by the roof rafters. However, the frequent absence of roof anchorage with the perimeter walls increased their susceptibility to toppling. In many cases, the internal wooden columns and beams have been proven to remain intact when the perimeter walls have failed (Fig 14b, Fig 15a). Well preserved LMSB-RC buildings (Fig 14c) exhibited a satisfactory behavior.

A negative case is the Agia Paraskevi church in Athani (Fig 15b): the RC ring beam-roof joist applied during rehabilitation and strengthening works has been proven to pose fatal burden on the stone bearing walls and the old deteriorated *pontelo*, which thereafter was not able to resist to roof gravity loads during the ground shaking. As a consequence, the monument of the eighteenth century collapsed, contrary to the LBSM-TC house of Fig 14b, where the timber frame managed to successfully bear the roof loading despite the failure of its external walls. The undesirable result of Agia Paraskevi church implies that erroneous

interventions and use of improper materials may impose increased risks, cancelling the effective seismic performance of the traditional architecture.

Finally, the collapse of an arbitrarily constructed tavern kiosk (Fig 15c), fortunately not in operation during winter months, emphasizes that life threats are pronounced whenever design and construction is not undertaken by experts.

## 6. Macroseismic field

In this section, we proceed to the assessment of the macroseismic field of the current earthquake and its comparison with the one of the 2003  $M_w = 6.2$  event. We use the European Macroseismic Scale [EMS-98, Grünthal, 1998] to estimate intensity for each of the 40 villages on the island using the SER damage protocol data. The EMS-98 approach, extensively used in Europe, emphasizes on the seismic performance of existing buildings. It incorporates definitions for various levels of damage for several types of structures providing a holistic damage assessment for a particular level of seismic intensity [Musson, 2000].

EMS-98 intensity estimates were based on the extent of damage (observed-to-registered) for the different building typologies (Fig 16). Macroseismic intensities of the two events (2003 and 2015) were assessed using similar quantitative criteria regarding the damage grade and typology. The color coding “Green-Yellow-Red” was correlated with the EMS-98 discrete damage grades as explained in Table 3. Given that the traditional LBSM-TF and LBSM-TC constructions are not contained in the EMS-98 guidelines, only LBSM and RC buildings were used with appropriate expert judgment and case-by-case considerations to assign sectoral intensities. Given the uncertainty of the SER data regarding the age of RC constructions, vulnerability class C was assumed for RC buildings with poor detailing and limited or absent ERD, most frequently found at the villages of the epicentral region. Our site survey confirmed that RC buildings prior to 1995 were the ones mainly affected within this typology. LSBM-RC typology was not included among the damaged structures.

Macroseismic intensities for the 2003 and 2015 earthquakes were obtained through a weighted mean approach, following Pomonis *et al.* [2014] and expert judgment on the validity of census data, the vulnerability (Table 2) and the damage classification scheme of Table 3. Comprehensive decisions have been made upon the quantitative definitions “few”, “many”, “most”, considering the data sparsity and the wide range of the statistical uncertainties. Secondary earthquake effects, such as damage caused by mutual pounding of adjacent buildings, landslides or slope failures, were not taken into account. Similarly, soil-structure interaction effects that may affect the vulnerability of the constructions have not been considered, since this issue is not within the scope of this work.

The analysis of the damage data of the 2015 earthquake presented in Fig 16b is summarized as follows: Intensity V (Strong) for no, or negligibly damaged areas; Intensity VI for sectors where few LBSM buildings suffered moderate damage and few RC suffered slight damage; Intensity VII for sectors with many LBSM and few RC buildings suffering moderate damage. Maximum intensity VIII has been concluded for the region of the SW peninsula, where a moderate-to-low percentage of LBSM buildings has been damaged. It should be noted that the intensity derived from the recording at VAS exceeds the observed macroseismic intensity in the same location. The EMS-98 intensity distribution for the 2003 earthquake presented in Fig 16a is in agreement with Karababa and Pomonis [2011] and Pomonis *et al.* [2014] although only integer intensity values have been assigned herein for compatibility reasons.

### 6.1. Fragility functions for LBSM buildings

The vulnerable conditions of a structure can be described using fragility and/or vulnerability functions. Fragility functions describe the probability of exceeding different limit states (such as damage states) given a level of ground shaking intensity, while vulnerability functions describe the probability of losses (such as economic losses) given a level of ground shaking. Refinement of the vulnerability estimates for the LBSM building category in terms of fragility curves has been made possible through the acquired damage observations of the two earthquakes in Lefkas Island (2003, 2015 earthquakes). For the 2003 earthquake, the dataset of Karababa and Pomonis [2011] was kindly provided by the authors. This is considered of prime importance toward the enrichment of the existing numerical or empirical formulations.

For this purpose, the macroseismic intensity EMS-98(MI) has been applied, even though it represents a circular procedure between damage, vulnerability and intensity definition, as instrumental data lack in spatial detail. The probability is obtained by applying a normal distribution fitting pattern among points of cumulative damage (ratio of buildings) and I(EMS-98) MI, described by the mean and a preset standard deviation per damage grade., using a linear regression. Standard deviation was considered equal to

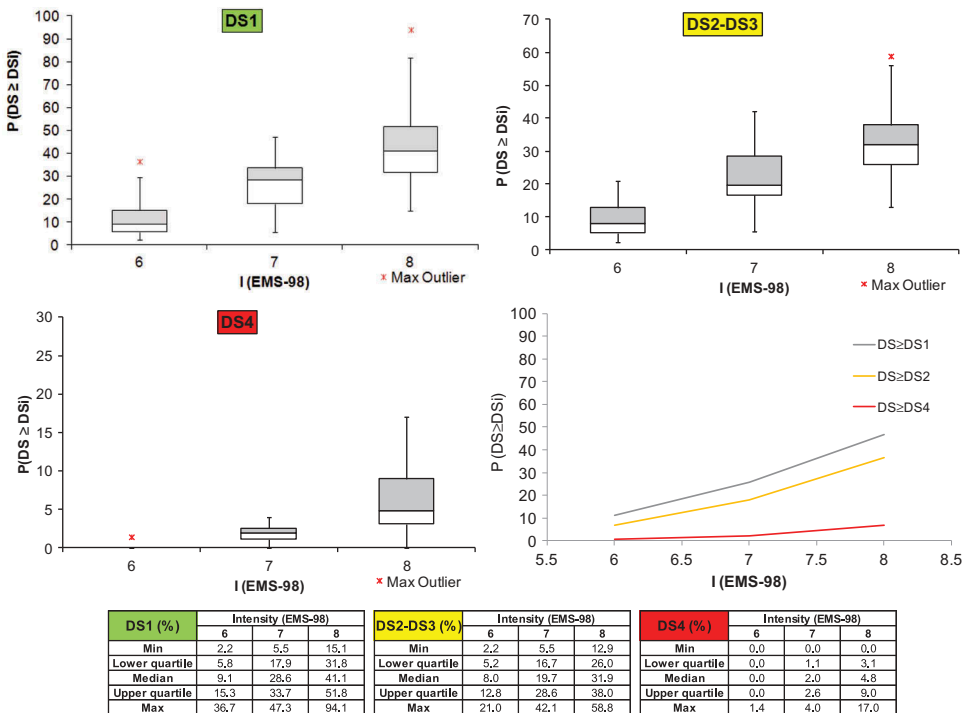


**Figure 17.** Empirical fragility box diagrams based on registered damage data to LBSM buildings from the 2003 and 2015 earthquakes. The vertical axis denotes the probability (P) that damage (D) exceeds a damage state (Di, i = 1–4). On each box, the central mark indicates the median, and the bottom and top edges of the box indicate the lower and upper quartiles (25th and 75th percentiles, respectively). The whiskers extend to the most extreme data points not considered outliers; outliers are plotted using the ‘\*’ symbol. Tables at the bottom indicate the probability values that define these intervals per Intensity measure. On the bottom right, the empirical fragility curves for the three equivalent damage states are plotted.



1.725 for all damage states, as suggested by Pomonis *et al.* [2014] for low variability of the seismic performance of the unreinforced masonry buildings.

Boxplots and tables of Fig 17 presenting the relation of damage states (DS1/“Green”, DS2-3/“Yellow”, DS4/“Red”) with respect to EMS-98 intensities provide a sense of the rather high variability of the available data. This variability is the main source of uncertainty, on top of the inherent procedure of defining the macroseismic intensity, based on subjective quantitative approximations. The dataset is considered of medium quality for a sufficient sample of surveyed buildings collected over a range of intensities, with few observational points per district [Rossetto *et al.*, 2013]. Therefore, the sampling frequency is considered acceptable, provided the accumulation of damage data from the two earthquakes. Coverage errors are treated by the use of census data and engineering judgment for the harmonization of the census and damage databases. Efforts for limitation of the measurement errors due to misclassification of the damage state were made by site surveys of the research team.

Fragility curves were then defined by applying a normal distribution fit between the cumulative damage (ratio of buildings) and  $I$  (EMS-98), described by the mean and an “*a priori*” standard deviation per damage grade (bottom right panel of Fig 17). Standard deviation was considered equal to 1.75 for all damage states, assuming low variability of the seismic performance for the LBSM buildings. The fragility curves are additionally defined by the following mean values:  $\mu_{DS \geq DS1} = 8.15$ ;  $\mu_{DS \geq DS2} = 8.61$ ;  $\mu_{DS \geq DS4} = 10.59$ .

## 7. Discussion and Conclusions

On November 17, 2015, an earthquake of magnitude 6.5 hit Lefkas Island in western Greece, related to the predominant CTF. The earthquake produced 2 human losses and few injuries, extensive environmental effects and moderate structural damage concentrated in the western part of the island. In monetary terms the earthquake cost about 20 million USD [Daniell *et al.*, 2015]. Fortunately, the event occurred this time of the year. If it had happened during the summer season, human loss could have been significant due to severe landslides and rock-falls that took place at the abrupt-narrow southwestern coast where the most popular/crowded beaches are located. Hereby, we present the macroseismic effects of this earthquake based on instrumental data and macroseismic observations.

Acceleration time histories at VAS station (Fig 1) located at a small epicentral distance ( $R = 6$  km) showed moderate ground motions. When considering the empirical relation of Skarlatoudis *et al.* [2003] and a source depth of 11 km, PGA extrapolated to the epicenter ( $R = 0$ ) equals  $382 \text{ cm/s}^2$  that reasonably explains the real recordings (max PGA = 0.36 g at the N-S component) and probably the low damage. Despite its larger magnitude, the current earthquake produced lower PGAs with respect to the 2014 Cephalonia earthquakes at a similar distance [Kassaras *et al.*, 2017]. Source radiation pattern is a possible explanatory feature, however, the lack of acceleration recordings of the mainshock apart from the LEF station located about 20 km away (Fig 1), does not allow association of ground motions with the observed damage at various locations.

Relatively high Arias intensity at VAS and intense displacement ( $\sim 0.4$  m) at the GNSS PONT advocate for extensive environmental effects observed along the western coast (Figure. 2). Structural damage mostly concentrated in the southwestern peninsula manifests spatial consistency with the results from InSAR interferometry [Melgar *et al.*, 2017]

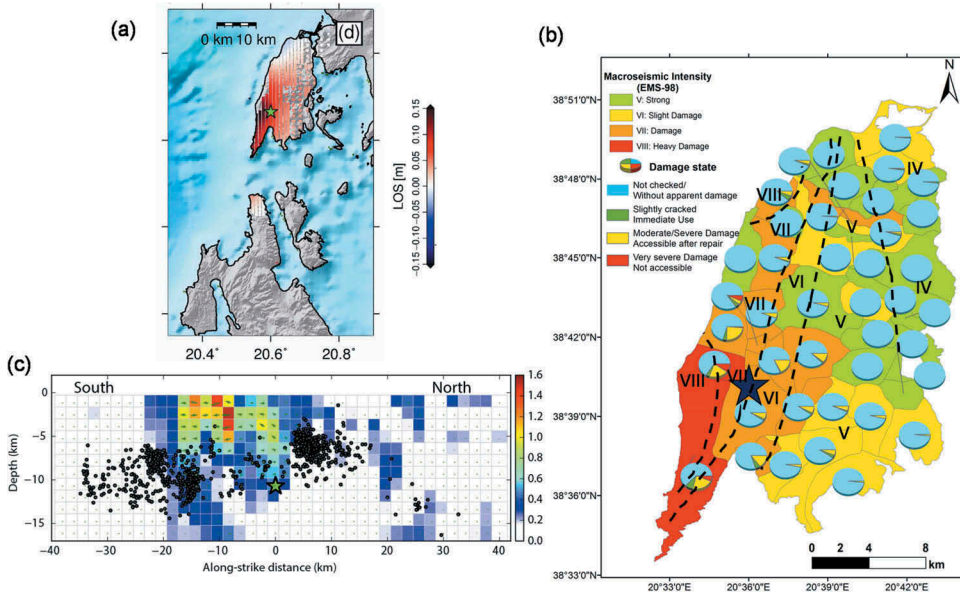


**Figure 18.** (a) Corrected ascending SAR line of sight (LOS) measurements [from Melgar *et al.*, 2017]; (b) Comparison between the distribution of structural damage and secondary effects. Dashed lines and Latin numbers indicate assessed ESI-07 [Michetti *et al.*, 2007], after Papathanassiou *et al.* [2017]. (c) Rupture slip from the joint inversion of GNSS, SAR and accelerometric data [from Melgar *et al.*, 2017]. Star indicates the location of the mainshock, black dots are aftershocks and the green arrows denote the direction of slip.

(Fig 18a) and the environmental intensities [Fig 18b, Papathanassiou *et al.*, 2017]. An additional source of damage is the shallow depth of the maximum slip, derived from the inversion of GNSS, InSAR and strong motion data, concentrated in the shallower part (< 5 km) of the southern patch of the causative fault (Fig 18c). The abovementioned highlight the effectivity of space geodesy as a damage monitoring system.

The herein damage inventory manifests structural consequences mainly concentrated within a 5 km radius around the epicenter, including villages with many traditional buildings of 6 different typologies (see section 4) which revealed: (a) satisfactory performance of the internal secondary timber load-bearing system for LBSM-TC, even after partial collapse of the external walls; (b) exceptional behavior for the LBSM buildings with ring beams (LBSM-RC) confirming that the accomplishment of box-action is crucial for masonry structures; (c) low damage at the LBSM-TF buildings, mainly concentrated at the masonry walls, (d) LBSM was proven to be the most vulnerable typology with 37.4% of its stock in the four most affected districts, yet with no collapse registered; (e) RC buildings responded elastically with localized damage imposed at times to structural elements with poor construction detailing and frequently to infill wall panels; (f) structural damage induced by ground deformation was also observed at the perimeter, retaining, or bearing walls.

Comparison with the effects of the 2003 earthquake demonstrates smaller structural damage for the 2015 event. Specifically, 14% of the total building stock was characterized as unsafe or dangerous due to the 2003 earthquake versus 3% in 2015. This difference is attributed to the location of the events with respect to the southward rupture propagation,

since the 2003 earthquake affected the whole island and dense urban areas, whilst the 2015 earthquake mainly impacted the sparsely inhabited southwestern part. In addition, typical buildings in the epicentral area of the 2015 earthquake, of low-to medium height (max. three story) with relatively small mass and low fundamental period [Karakostas *et al.*, 2005], were not heavily stressed, due to the particular shape of the response spectrum of the mainshock (Fig 3f). However, the vertical component, of almost the same amplitude as the E-W horizontal one, may have had a contribution to the damage near the epicenter due to its low predominant period (0.1 s). Thereafter, interventions performed after the  $M_w = 6.2$  earthquake in 2003, widely seen during our field surveys, likely contributed to the structural enhancement of buildings leading to a better seismic performance.

With the aid of literature and qualitative observations, EMS-98 vulnerability was estimated for the structural typologies recognized on site. The EMS-98 intensity, based on the analysis of damage data and vulnerability estimates resulted in a maximum value of VIII in the two most affected districts of Athani and Dragano (see Fig 2), fortunately a sparsely populated area. The intensity decays to the northeast, consistently with the rupture slip distribution (Fig 18a,b). For compatibility purposes, macroseismic intensities for the 2003  $M_w = 6.2$  event [Karababa and Pomonis, 2011] were re-assessed on the basis of the same assumptions as for the 2015 earthquake, yielding maximum intensity IX for the capital of Lefkada (LEF, see Fig 1). The outcome of this analysis is empirical fragility curves for the most common LBSM typology in Lefkas from cumulative damage data of the two earthquakes (2003 and 2015, Fig 17). These curves, are tentatively to be of use for further investigations, acknowledging the uncertainties and potential biases the available dataset may impose.

In the seismic-prone areas of Greece, local stakeholders and citizens are more alert about the earthquake implications, and take proper measures, design and building practices that further enhance the actual seismic capacity of the buildings, beyond the expected one from the analytical investigations. In Lefkas, the need to adopt more earthquake resistant techniques was recognized some hundreds of years ago and, thus, the double *pontelo* structural system, being a state-of-the-art technique of supreme seismic performance and the “triple level” foundation system were born. Considering the overall satisfactory response of the non-engineered constructions to the loads of the current earthquake, we acknowledge the above concepts together with the quality of applied construction materials and workmanship. Therefore, we recommend measures for their protection and restoration, and further study on their seismic properties by analytic methodologies toward modern applications.

## Acknowledgments

We acknowledge the waveform data provided by NOA and EPPO-ITSAK. We are thankful to local authorities and people of Lefkas for facilitating our effort during our surveys. We would like to express our gratefulness to D. Ktenas, A. Monachi, P. Korfiatis, E. Frangoulis, G. Karambalis, G. Katopodis, A. Bariamis and A. Soldatos. We warmly thank E. Vintzileou, G. Papathanassiou, C. Tsimi, E. Kollia for discussions. We thank J. Geng who processed the 1-Hz GPS data from station PONT, F. Karababa for providing the 2003 damage data, D. Kalantoni for making available photographic material of the buildings, J. Maxant and H. Yesou for processing satellite imagery. Instrumental time-series were pre-processed using SAC2000 [Goldstein *et al.*, 2003]. Fig 1 was produced using the GMT software [Wessel and Smith, 1991]. Particle motion diagrams of Fig 2 were plotted using the GEOPSY software [SESAME, 2005].

## References

- Afshari, K. and Stewart, J. [2016]. “Physically parametrized prediction equations for significant duration in active crustal regions”. *Earthquake Spectra* **32**(4), 2057–2081. doi:10.1193/063015EQS106M.
- Anagnostopoulos, S. and Moretti, M. [2008]. “Post-earthquake emergency assessment of building damage, safety and usability”. *Part 1: Technical Issues, Soil Dynamics and Earthquake Engineering* **28**, 223–232.
- Arias, A. A. [1990]. “Measure of earthquake intensity,” in *Seismic Design for Nuclear Power Plants*, ed. R. J. Hansen (Massachusetts Institute of Technology Press, Cambridge, MA), pp. 438–483.
- Avallone, A., Cirella, A., Cheloni, D., Tolomei, C., Theodoulidis, N., Piatanesi, A., Briole, P. and Ganas, A. [2017]. “Near-source high-rate GPS, strong motion and InSAR observations to image the 2015 Lefkas (Greece) Earthquake rupture history”. *Scientific Reports* **7**, doi:10.1038/s41598-017-10431-w.
- Benetatos, C., Dreger, D. and Kiratzi, A. [2007]. “Complex and Segmented Rupture Associated with the 14 August 2003 Mw 6.2 Lefkas, Ionian Islands, Earthquake”. *Bulletin of the Seismological Society of America* **99**(6), No. 1B 35–51. doi:10.1785/0120060123.
- Benetatos, C., Kiratzi, A., Roumelioti, Z., Stavrakakis, G., Drakatos, G. and Latoussakis, I. [2005]. “The 14 August 2003 Lefkas Island (Greece) earthquake: focal mechanisms of the mainshock and of the aftershock sequence”. *Journal of Seismology* **9**(2), 171–190. doi:10.1007/s10950-005-7092-1.
- Bommer, J., Magenes, G., Hancock, J. and Penazzo, P. [2004]. “The Influence of Strong-Motion Duration on the Seismic Response of Masonry Structures”. *Bulletin of Earthquake Engineering* **2**, 1–26. doi:10.1023/B:EEEE.0000038948.95616.bf.
- Bommer, J. J., Stafford, P. J. and Alarcón, J. E. [2009]. “Empirical equations for the prediction of the significant, bracketed, and uniform duration of earthquake ground motion”. *Bulletin of the Seismological Society of America* **99**(6), 3217–3233. doi:10.1785/0120080298.
- Cen, E. N. 1998-1 [2004] “Eurocode 8. *Design of Structures for Earthquake Resistance*”, European Committee for Standardization, Brussels.
- Chousianitis, K., Del Gaudio, V., Kalogeras, I. and Ganas, A. [2014]. “Predictive model of Arias intensity and Newmark displacement for regional scale evaluation of earthquake-induced landslide hazard in Greece”. *Soil Dynamics and Earthquake Engineering* **65**, 11–29. doi:10.1016/j.soildyn.2014.05.009.
- Chousianitis, K., Konca, O., Tselentis, A., Papadopoulos, G. and Gianniu, M. [2016]. “Slip model of the 17 November 2015 Mw=6.5 Lefkas earthquake from the joint inversion of geodetic and seismic data”. *Geoph. Research Letters* **43**(15), 7973–7981. doi:10.1002/2016GL069764.
- Daniell, J., Schäfer, A., Pomonis, A., Mühr, B. and Wenzel, F. [2015] “CEDIMM Forensic Disaster Analysis – 2015 Lefkas, Greece Earthquake”, Report No.1, CATDAT, [CATNews&Earthquake-report.com](http://CATNews&Earthquake-report.com).
- EAK-2000. [2003] “*Greek National Building Code*”, Earthquake Protection and Planning Organization of Greece (OASP) EPPO Publications, Athens.
- Ganas, A., Elias, P., Papathanasiou, G., Avallone, A., Papastergios, A., Valkaniotis, S., Parcharidis, I. and Briole, P. [2016]. “Coseismic deformation, geo-environmental effects and seismic fault of the 17 November 2015 M=6.5, Lefkas Island, Greece earthquake”. *Tectonophysics* **687**, 201–222. doi:10.1016/j.tecto.2016.08.012.
- Goldstein, P., Dodge, D., Firpo, M. and Minner, L. [2003] “SAC2000: signal processing and analysis tools for seismologists and engineers”, The IASPEI International Handbook of Earthquake and Engineering Seismology, WHK Academic Press, London.
- Grünthal, G. ed. [1998] “*European Macroseismic Scale 1998, Cahiers Du Centre Européen De Géodynamique Et De Séismologie 15*”, Europ. Center for Geodyn. and Seism, Luxembourg.
- Hatzfeld, D., Kassaras, I., Panagiotopoulos, D. G., Amorese, D., Makropoulos, K., Karakaisis, G. F. and Coutant, O. [1995]. “Microseismicity and strain pattern in Northwestern Greece”. *Tectonics* **14**, 773–785. doi:10.1029/95TC00839.
- Ilieva, M., Briole, P., Ganas, A., Dimitrov, D., Elias, P., Mouratidis, A. and Charara, R. [2016]. “Fault plane modelling of the 2003 August 14 Lefkas Island (Greece) earthquake based on the

- analysis of ENVISAT SAR interferograms”. *Tectonophysics* **693**, 47–65. doi:10.1016/j.tecto.2016.10.021.
- Kahle, H. G., Müller, M., Geiger, A., Danuser, G., Mueller, S., Veis, G., Billiris, H. and Paradissis, D. [1995]. “The strain field in northwestern Greece and the Ionian Islands: results inferred from GPS measurements”. *Tectonophysics* **249**(1), 41–52. doi:10.1016/0040-1951(95)00042-L.
- Kalantoni, D. [2016] “Development of empirical seismic risk models in the old town of Lefkas”, PhD Thesis, National and Kapodistrian University of Athens.
- Kalantoni, D., Pomonis, A., Kassaras, I., Kouskouna, V., Pavlou, K., Vassilopoulou, S., Karababa, F. and Makropoulos, K. [2013] “Vulnerability assessment in Lefkas old town (W. Greece) with the use of EMS-98; comparison with the 14-8-2003, Mw= 6.2, earthquake effects. First results”, Proc. of Vienna Congress on Recent Advances in Earthquake Engineering and Structural Dynamics (VEESD 2013), 28-30 August 2013, Vienna, Austria, Paper No. 356
- Karababa, F. and Pomonis, A. [2011]. “Damage data analysis and vulnerability estimation following the August 14, 2003 Lefkas Island, Greece”. *Bulletin of Earthquake Engineering* **9**, 1015–1046. doi:10.1007/s10518-010-9231-5.
- Karakonstantis, A. and Papadimitriou, P. [2010] “Earthquake relocation in Greece using a unified and homogenized seismological catalogue”, Bull. Geol. Soc. Greece, *Proc. of the 12th International Congress*, May 2010, Patras, Greece, 2043–2052. doi:10.12681/bgsg.11394.
- Karakostas, C., Lekidis, V., Makarios, T., Salonikios, T., Sous, I. and Demosthenous, M. [2005]. “Seismic response of structures and infrastructure facilities during the Lefkas, Greece earthquake of 14/8/2003”. *Engineering Structures* **27**, 213–227. doi:10.1016/j.engstruct.2004.09.009.
- Kassaras, I., Kalantoni, D., Benetatos, C., Kaviris, G., Michalaki, K., Sakellariou, N. and Makropoulos, K. [2015]. “Seismic damage scenarios in Lefkas old town (W. Greece)”. *Bulletin of Earthquake Engineering* **13**, 799–825. doi:10.1007/s10518-014-9643-8.
- Kassaras, I., Kalantoni, D., Pomonis, A., Kouskouna, V., Karababa, F. and Makropoulos, K. [2014]. “Development of seismic damage scenarios in Lefkas old town (W. Greece): part I—vulnerability assessment of local constructions with the use of EMS-98”. *Bulletin of Earthquake Engineering*. **13**, 799–825. doi:10.1007/s10518-014-9643-8.
- Kassaras, I., Kapetanidis, V. and Karakonstantis, A. [2016]. “On the spatial distribution of seismicity and the 3D tectonic stress field in western Greece”. *Physics and Chemistry of the Earth* **95**, 50–72. doi:10.1016/j.pce.2016.03.012.
- Kassaras, I., Papadimitriou, P., Kapetanidis, V. and Voulgaris, N. [2017]. “Seismic site characterization at the western Cephalonia Island in the aftermath of the 2014 earthquake series”. *International Journal of Geo-Engineering* **8**(7), doi:10.1186/s40703-017-0045-z.
- Kazantzidou-Firtinidou, D., Kassaras, I., Tonna, S., Ganas, A., Vintzileou, E. and Chesi, C. [2016] “The November 2015 Mw6.4 earthquake effects in Lefkas Island”, *Proc. of 1st ICONHIC*, Crete, Paper No 119.
- Louvari, E., Kiratzi, A. and Papazachos, B. C. [1999]. “The Cephalonia Transform Fault and its extension to western Lefkas Island (Greece)”. *Tectonophysics* **308**(1–2), 223–236. doi:10.1016/S0040-1951(99)00078-5.
- Makarios, T. and Demosthenous, M. [2008] “The Traditional Buildings of Lefkas with double Bearing system and their seismic behavior”, *Proc. of the 3rd Greek Conference on Earthquake Engineering and Technical seismology*, November 5-7, 2008, Athens.
- Makropoulos, K., Kaviris, G. and Kouskouna, V. [2012]. “An updated and extended earthquake catalogue for Greece and adjacent areas since 1900”. *Natural Hazards Earth System Sciences* **12**, 1425–1430. doi:10.5194/nhess-12-1425-2012.
- Malakasis, D. [2000] “The old Houses of Lefkas, 1850-1920”, Edn. Fagotto/Throisma (in Greek).
- Melgar, D., Ganas, A., Geng, J., Liang, C., Fielding, E. J. and Kassaras, I. [2017]. “Source characteristics of the 2015 Mw6.5 Lefkas, Greece, strike-slip earthquake”. *Journal of Geophysical Research* **122**(3), 2260–2273.
- Michetti, A. M., Esposito, E., Guerrieri, L., Porfido, S., Serva, L., Tatevossian, R., Vittori, E., Audemard, F., Azuma, T., Clague, J., Comerci, V., Gürpınar, A., Mc Calpin, J., Mohammadioun, B., Mörner, N. A., Ota, Y. and Roghazin, E. [2007]. “Intensity Scale ESI, 2007”, in *Memorie Descrittive Carta Geologica*



- d'Italia*, Eds. L. Guerrieri and E. Vittori (APAT, Servizio Geologico d'Italia— Dipartimento Difesa del Suolo, Rome, Italy), 53–74.
- Musson, R. [2000]. “Intensity-based seismic risk assessment”. *Soil Dynamics Earthquake Engineering* **20**, 353–360. doi:10.1016/S0267-7261(00)00083-X.
- National Statistical Service of Greece (NSSG) [2001] “Results of plots and building census on March 2001”, [www.statistics.gr](http://www.statistics.gr).
- National Statistical Service of Greece (NSSG) [2011] “Results of plots and building census on February/May 2011”, [www.statistics.gr](http://www.statistics.gr).
- Papadatou-Giannopoulou, C. [1999] “*Lefkas Researching*”, Editions Achaïkes, Patras, Greece (in Greek).
- Papadatou-Giannopoulou, C. [2014] “*Stability Techniques of the Traditional Architecture and Idiomatic Dictionary of Lefkas. Lefkas Researching*”, Editions Achaïkes, Patras (in Greek).
- Papadimitriou, E., Karakostas, V., Mesimeri, M., Chouliaras, G. and Ch., Kourouklas. [2017]. “The Mw6.5 17 November 2015 Lefkas (Greece) Earthquake: structural interpretation by means of the aftershock analysis”. *Pure Appl. Geophys.* **174**(10), 3869–3888. doi:10.1007/s00024-017-1601-3.
- Papathanassiou, G., Pavlides, S. and Ganas, A. [2005]. “The 2003 Lefkas earthquake: field observations and preliminary microzonation map based on liquefaction potential index for the town of Lefkas”. *Engineering Geology* **82**, 12–31. doi:10.1016/j.enggeo.2005.08.006.
- Papathanassiou, G., Valkaniotis, S., Ganas, A., Grendas, N. and Kollia, E. [2017]. “The November 17th, 2015 Lefkas (Greece) strike-slip earthquake: field mapping of generated failures and assessment of macroseismic intensity ESI-07”. *Engineering Geology* **220**, 13–30. doi:10.1016/j.enggeo.2017.01.019.
- Papathanassiou, G., Valkaniotis, S., Ganas, A. and Pavlides, S. [2013]. “GIS-based statistical analysis of the spatial distribution of earthquake-induced landslides in the island of Lefkas, Ionian Islands, Greece”. *Landslides* **10**, 771–783. doi:10.1007/s10346-012-0357-1.
- Papazachos, B. and Papazachou, C. [2003] “*The Earthquakes of Greece*” 3rd, Ziti Public, Thessaloniki, Greece.
- Pomonis, A., Gaspari, M. and Karababa, F. [2014]. “Seismic vulnerability assessment for buildings in Greece based on observed damage datasets”. *Bollettino Di Geofisica Teorica Ed Applicata* **55**, 501–534.
- Rossetto, T., Ioannou, I. and Grant, D. N. [2013] “Existing empirical fragility and vulnerability functions: compendium and guide for selection”, *GEM Technical Report 2013-X*, GEM Foundation, Pavia, Italy. [www.globalquakemodel.org](http://www.globalquakemodel.org)
- Saltogianni, V., Gianniou, M., Moschas, F. and Stiros, S. [2016]. “Pattern of dynamic displacements in a strike-slip earthquake”. *Geophys. Res. Lett.* **43**, 6861–6868. doi:10.1002/2016GL069507.
- Seismosoft [2016] “SeismoSignal 2016 – A computer program for signal processing of strong-motion data”, available from <http://www.seismosoft.com>.
- SESAME [2005] “Guidelines for the implementation of the H/V spectral ratio technique on ambient vibrations measurements, processing and interpretations”, SESAME European research project EVG1-CT-2000–00026, deliverable D23.12.
- Skarlatoudis, A. A., Papazachos, C. B., Margaris, B. N., Theodoulidis, N. T. and Papaioannou, C. [2003]. “Empirical peak ground-motion predictive relations for shallow earthquakes in Greece”. *Bull. Seism. Soc. Am.* **93**(6), 2591–2603. doi:10.1785/0120030016.
- Sokos, E., Zahradnik, J., Gallovič, F., Serpetsidaki, A., Plicka, V. and Kiratzi, A. [2016]. “Asperity break after 12 years: the Mw6.4 2015 Lefkas (Greece) earthquake”. *American Geoph. Res. Lett.* **43**, 6137–6145. doi:10.1002/2016GL069427.
- Sorel, D., Nesteroff, W. D., Limond, J., Lemeille, F. and Sebrier, M. [1976]. “Mise en évidence de structures compressives sous-marine plio-pleistocène dans l’arc égeen externe au Large de Lefkas (Isles Ioniennes, Grèce)”. *Académie Des Sciences Comptes Rendus* **282**, 2045–2048. Paris
- Stucchi, M., Rovida, A., Gomez Capera, A. A., Alexandre, P., Camelbeeck, T., Demircioglu, M. B., Gasperini, P., Kouskouna, V., Musson, R. M. W., Radulian, M., Sesetyan, K., Vilanova, S., Baumont, D., Bungum, H., Fäh, D., Lenhardt, W., Makropoulos, K., Martinez Solares, J. M., Scotti, O., Zivcic, M., Albini, P., Batllo, J., Papaioannou, C., Tatevossian, R., Locati, M., Meletti, C., Vigano, D. and Giardini, D. [2013]. “The SHARE European earthquake catalogue (SHEEC) 1000–1899”. *Journal of Seismology* **17**(2), 523–544. doi:10.1007/s10950-012-9335-2.

- Tonna, S. [2014] “Resistere ai terremoti: l’esperienza nei sistemi costruttivi dell’architettura tradizionale”, PhD Thesis in Preservation of Architectural Heritage, Politecnico di Milano (in Italian).
- Tonna, S., Chesi, C., Vintzileou, E. and Katopodis, K. [2014]. “Traditional building criteria on the island of Lefkas: peculiarities of the foundation system,” in *Proc. Of SAHC2014 – 9th International Conference on Structural Analysis of Historical Constructions*, eds.F. Peña and M. Chávez (14–17 October 2014, Mexico City, Mexico), pp. 10.
- Tonna, S. and Chesi, C. [2016]. “A multidisciplinary approach to the analysis of the traditional Lefkas houses,” in *Historical Earthquake-Resistant Timber Framing in the Mediterranean Area HEaRT 2015*, eds. H. Cruz *et al* (Springer International Publishing, Switzerland), pp. 147–157.
- Tonna, S. and Chesi, C. [2015] “Implications of earthquake return periods on the building quality”, *Proc. of The XII International Forum “Le vie dei Mercanti”*, Best practice in Heritage conservation and management, Aversa and Capri, Italy.
- Touliatos, P. and Vintzileou, E. [2006] “Seismic behavior of the structural system in the historic town of Lefkas”, *Proc. of 15th Reinforced Concrete Congress*, TEE, ETEK, Alexandroupolis, Greece, pp. 1–12.
- Trifunac, M. D. and Westermo, B. D. [1982]. “Duration of strong earthquake shaking”. *Soil Dynamics and Earthquake Engineering* **1**(3), 117–121. doi:10.1016/0261-7277(82)90002-X.
- Tselentis, G. and Danciu, L. [2008]. “Empirical relationships between modified Mercalli intensity and engineering ground-motion parameters in Greece”. *Bulletin of the Seismological Society of America* **98**(4), 1863–1875. doi:10.1785/0120070172.
- Vintzileou, E., Touliatos, P., Zeris, C., Repapis, K., Zagotsis, A., Leonardos, E., Palieraki, V. and Adami, C. [2007a], “Lefkas seismic construction”. EPPO, NTUA, Lefkas’s Municipality Library (in Greek).
- Vintzileou, E., Zagotsis, A., Repapis, C. and Zeris, C. [2007b]. “Seismic behavior of the historical structural system of the island of Lefkas, Greece”. *Construction and Building Materials* **21**, 225–236. doi:10.1016/j.conbuildmat.2005.04.002.
- Wells, D. L. and Coppersmith, K. J. [1994]. “New empirical relationships among magnitude, rupture length, rupture width, rupture area, and surface displacement”. *Bulletin of the Seismological Society of America* **84**(4), 974–1002.
- Wessel, P. and Smith, W. H. F. [1991]. “Free software helps map and display data. EOS, Transactions”. *American Geophysical Union* **72**, 441–448. doi:10.1029/90EO00319.
- Zahradník, J. and Sokos, E. [2015] “Lefkas 17/ 11/2015,Mw 6.4 event: quick estimate of source complexity”, Report sent to EMSC on 22/11/2015, <http://www.emsc-csem.org/Files/event/470390>.



## Appendix A

**Table A1.** Registered damage per sector and structural typology, after the post-seismic survey by SER. Percent number is per 2011 census data apart from Mixed buildings. When marked "Incop." Incompatibility between the damage and census databases is observed. The location of some of the districts is presented in Fig 2.

District	I (EMS-98)	Yellow					Red					Total number		
		RC	RC %	LBSM	LBSM %	Mixed	Mixed % (per 2001)	RC	RC %	LBSM	LBSM %		Mixed	Mixed % (per 2001)
Lefkas	6	15	0.64	16	12.90	4	0.7%	0	0.00	0	0.00	0	0.0%	3616
Tsoukalades	5	1	0.33	1	0.48	0	0.0%	0	0.00	0	0.00	0	0.0%	636
Apalpaini	6	0	0.00	3	6.82	0	0.0%	0	0.00	0	0.00	0	0.0%	409
Karriotes	5	0	0.00	0	0.00	0	0.0%	0	0.00	0	0.00	0	0.0%	291
Karya	6	1	0.34	13	3.33	0	0.0%	0	0.00	0	0.00	0	0.0%	746
Agios Nikitas	7	3	2.08	6	28.57	1	14.3%	0	0.00	0	0.00	0	0.0%	165
Kalamitsi	5	1	0.43	1	2.22	0	0.0%	0	0.00	0	0.00	0	0.0%	288
Exantheia	7	3	3.30	11	5.47	3	75.0%	0	0.00	0	0.00	0	0.0%	325
Pigadisanoi	5	0	0.00	1	1.56	1	Incop.	0	0.00	0	0.00	0	0.0%	142
Alexandros	5	1	0.17	0	0.00	0	0.0%	0	0.00	0	0.00	0	0.0%	776
Egklouvi	5	0	0.00	3	1.85	0	0.0%	0	0.00	0	0.00	0	0.0%	220
Komilio	7	1	1.67	18	52.94	4	Incop.	0	0.00	0	0.00	1	50.0%	94
Chortata	7	0	0.00	7	7.95	3	9.4%	0	0.00	0	0.00	0	0.0%	188
Nydri	5	2	0.37	0	0.00	0	0.0%	0	0.00	0	0.00	0	0.0%	699
Agios Ilias	7	1	2.22	10	11.24	3	50.0%	0	0.00	0	0.00	0	0.0%	134
Nikolis	7	5	7.69	11	9.73	4	Incop.	0	0.00	3	2.65	3	100.0%	182
Vlychos	5	0	0.00	1	0.72	0	0.0%	0	0.00	0	0.00	0	0.0%	441
Dragano	8	8	17.39	11	13.92	9	60.0%	0	0.00	12	15.19	0	0.0%	125
Charadiatika	5	0	0.00	0	0.00	0	0.0%	0	0.00	0	0.00	0	0.0%	254
Agios Petros	7	13	2.53	37	38.14	11	6.3%	0	0.00	9	9.28	1	0.5%	749
Athani	8	15	12.71	28	19.18	10	30.3%	0	0.00	18	12.33	0	0.0%	264
Vournika	6	0	0.00	8	8.79	2	Incop.	0	0.00	0	0.00	0	0.0%	166
Syvros	7	1	1.61	26	14.53	0	0.0%	0	0.00	0	0.00	1	5.6%	326
Katochori	5	0	0.00	1	0.82	0	0.0%	0	0.00	0	0.00	0	0.0%	209
Fterno	6	0	0.00	6	4.72	0	0.0%	0	0.00	0	0.00	0	0.0%	247
Poros	6	0	0.00	5	7.58	0	0.0%	0	0.00	0	0.00	0	0.0%	245

<i>Marantochori</i>	6	2	0.86	12	10.91	2	Incop.	0	0.00	0	0.00	0	0.00	0.00	396
<i>Kontariani</i>	6	0	0.00	4	5.63	0	0.0%	0	0.00	0	0.00	0	0.00	0.0%	157
<i>Vasiliki</i>	7	15	7.54	27	27.84	1	3.0%	0	0.00	3	3.09	0	0.00	0.0%	328
<i>Eygiros</i>	6	0	0.00	4	2.74	0	0.0%	0	0.00	0	0.00	0	0.00	0.0%	336
<i>Kavalos</i>	5	0	0.00	1	0.61	0	0.0%	0	0.00	0	0.00	0	0.00	0.0%	225
<i>Asprogerakata</i>	7	1	1.43	1	1.61	0	0.0%	0	0.00	0	0.00	0	0.00	0.0%	139
<i>Spanochori</i>	5	0	0.00	0	0.00	0	0.0%	0	0.00	0	0.00	0	0.00	0.0%	187
<i>Lazarata</i>	7	5	3.85	5	2.92	1	2.4%	0	0.00	0	0.00	0	0.00	0.0%	324
<i>Pinakochori</i>	6	1	1.67	7	6.80	0	0.0%	0	0.00	0	0.00	0	0.00	0.0%	165